

**RHEOLOGICAL CHARACTERISATION OF
SILVER (Ag) BASED ISOTROPIC
CONDUCTIVE ADHESIVES**

By

KAU CHEE LEONG

A dissertaton submitted to the Department of Mechanical and Material
Engineering
Lee Kong Chian Faculty of Engineering and Science
UniversitiTunku Abdul Rahman
in partial fulfilment of the requirements for the degree of
Master of Engineering Science
March 2016

ABSTRACT

RHEOLOGICAL CHARACTERISATION OF SILVER (Ag) BASED ISOTROPIC CONDUCTIVE ADHESIVES

Kau Chee Leong

Tin–lead solder alloys are widely used in the electronic industry. They serve as interconnects that provide the conductive path required to achieve connection from the chip to the substrate. There are increasing concerns with the use of tin–lead alloy solders in recognition of hazards posed by lead to the eco-system. Isotropic conductive adhesives (ICAs) have been considered as the most promising alternatives of tin-lead solder due to lower processing temperature and volatile organic compound. As the current product miniaturisation trends continue for hand-held consumer products, area array type package solutions are now being designed into products. The assembly of these devices requires the printing or dispensing of very small volume of isotropic conductive adhesives (ICAs) deposits consistently from pad to pad, and from board to board.

Rheology is the study of flow characteristic and understanding the behaviour of the particular substance. The rheological characterisation of isotropic conductive adhesives pastes is an important in formulating a material that will flow accordingly when printed or dispensed. This will ultimately reduce common defects such as bridging and open circuits, which will lead to

increase in yield in the assembly of electronic devices.

The works reported here on the rheological characterisation of silver flakes and mixture of silver flakes and silver nano-powder based ICAs paste used in electronic assembly applications. The study found that the thixotropic behaviour of the pastes changes with the introduction of silver nano-powder. The pastes with silver nano-powder exhibited higher viscosity, highly thixotropic in nature and a good recovery index at 0.6 wt% and 0.8 wt%. The creep-recovery study showed that the pastes with silver nano-powder exhibited higher deformation at 0.8 wt% and poor recovery. In the oscillatory study, the ICAs with nano-particle showed have higher $G' = G''$ value and higher storage modulus, G' .

ACKNOWLEDGEMENT

First and foremost, I would like to express my sincere appreciation and deepest gratitude to my supervisor, **Professor Dr. Rajkumar Durairaj** for the useful comments, remarks and engagement through the learning process of this master dissertation. His guidance helped me in all the time of research and writing of this dissertation. I could not have imagined having a better advisor and mentor for my Master study.

Furthermore, I would also like to acknowledge with much appreciation the crucial role of the staff of UTAR lab who gave the permission to use all required equipments and the necessary materials to complete the task.

I would like to acknowledge course mates for giving me support and advise all the way. A special thanks goes to my teammate, who help me to assemble the parts and gave suggestion about the task.

Last but notleast; I would like to thank my family: my parents Mr Kau See Aha and Mdm. Ng SauKheng, for giving birth to me at the first place and supporting me spiritually throughout my life.

APPROVAL SHEET

This thesis entitled “**RHEOLOGICAL CHARACTERISATION OF SILVER (Ag) BASED ISOTROPIC CONDUCTIVE ADHESIVES**” was prepared by **KAU CHEE LEONG** and submitted as partial fulfilment of the requirements for the degree of Master of Engineering Science at UniversitiTunku Abdul Rahman.

Approved by:

(Associate Professor Dr. Rajkumar Durairaj)

Date:

Supervisor

Department of Mechanical and Material Engineering

Faculty of Engineering Science

UniversitiTunku Abdul Rahman

FACULTY OF ENGINEERING AND SCIENCE
UNIVERSITI TUNKU ABDUL RAHMAN

Date: 29th February 2016

SUBMISSION OF THESIS

It is hereby certified that **KAU CHEE LEONG** (ID No: **09UEM09096**) has completed this thesis entitled “**RHEOLOGICAL CHARACTERISATION OF SILVER (Ag) BASED ISOTROPIC CONDUCTIVE ADHESIVES**” under the supervision of Professor Dr. Rajkumar Durairaj(Supervisor) from the Department of Mechanical and Material Engineering, Faculty of Engineering and Science.

I understand that the University will upload softcopy of my thesis in pdf format into UTAR Institutional Repository, which may be made accessible to UTAR community and public.

Yours truly,

(KAU CHEE LEONG)

DECLARATION

I hereby declare that the dissertation is based on my original work except for quotations and citations, which have been duly acknowledged. I also declare that it has not been previously or concurrently submitted for any other degree at UTAR or other institutions.

Name _____

(KAU CHEE LEONG)

Date _____

LIST OF PUBLICATION

1. R. Durairaj and **KauChee Leong**, “Effect of Silver Flakes and Particle Shape on the Steady Shear Viscosity of Isotropic Conductive Adhesives”, Journal of Testing and Evaluation, Vol. 43, No. 6, Month 2014. DOI: 10.1520/JTE20130084. (ISI Cited Publication)
2. R. Durairaj, **KauChee Leong**, L.Chiawea and Wong MeeChu(2010). Thixotropic Behaviour of Nano-composite pastes (Nikel and Platinum power) Malaysian Science and Technology Congress (MSTC) 2010
3. R. Durairaj*, L. Chiawea, Lam Wai Man, **KauCheeLeong**and Wong Mee Chu. Investigation of the Thixotropic Behaviour of Solder Pastes and Isotropic Conductive Adhesives Used in The Assembly of High Density Electronic Packing Malaysian Science and Technology Congress (MSTC) 2010
4. R. Durairaj, **KauChee Leong**, L.Chiawea and Wong Mee Chu. Oscillatory And Creep Recovery Test On Nano-composite Lead-Free Solder Pastes (Nickel and Platinum Power)8th International Conference On Composite Science And Technology Kuala Lumpur 2011
5. R. Durairaj, Lim Chia Wea, **KauCheeLeong** , Wong Mee Chu and Liang MengSuan. Rheology and Processing of Ni based Nano-Composite Pastes for Electronic Assembly. 8th International Conference On Composite Science And Technology Kuala Lumpur 2011.
6. “Rheology - New Concepts, Applications and Methods”
Chapter 2 Rheological Characterisation of Diglycidylether of Bisphenol-A (DGEBA) and Polyurethane (PU) Based Isotropic Conductive Adhesives
By R. Durairaj, Lam Wai Man, **KauChee Leong**, LiewJian Ping, N. N. Ekere and Lim SeowPhengIntech Publication

TABLE OF CONTENTS

	Page
ABSTRACT	ii
ACKNOWLEDGEMENTS	iv
APPROVAL SHEET	v
SUBMISSION OF THESIS	vi
DECLARATION	vii
LIST OF PUBLICATION	viii
TABLE OF CONTENTS	ix
LIST OF TABLES	xiii
LIST OF FIGURES	xv
LIST OF ABBREVIATIONS	xix
CHAPTER	
1.0 INTRODUCTION	1
1.1 Research Background	1
1.2 Problem Statement and Research Objectives	2
1.3 Overview	4
2.0 LITERATURE REVIEW	5
2.1 Introduction	5
2.2 Rheology of Pastes	6
2.3 Visco-elastic and Thixotropic Behaviour in Paste Suspension	11
.	11

2.3.1	Visco-elastic Behaviour of Paste Suspensions	12
2.3.2	Thixotropic Behaviour in Paste Suspensions	14
3.0	RHEOLOGY	18
3.1	Rheology	18
3.2	Basic terms associated with Rheology	19
3.2.1	Viscosity	19
3.2.2	Shear Rate	21
3.2.3	Shear Stress	22
3.3	Viscous Fluids	22
3.3.1	Newtonian Fluids	22
3.3.2	Non-Newtonian Fluids	23
3.3.2.1	Pseudoplastic	24
3.3.2.2	Shear Thickening	26
3.3.2.3	Yield Stress Behaviour	27
3.4	Thixotropy	30
3.5	Visco-elasticity	33
3.5.1	Oscillatory Test	34
3.5.2	Creep-recovery Test	37
3.6	Correlation of viscosity with volume fraction	38
4.0	MATERIALS AND METHODS	41
4.1	Introduction	41

4.2	Introduction to Isotropic Conductive Adhesives (ICAs)	41
4.3	Materials and sample preparation	42
4.4	Rheometry	45
	4.4.1 Viscometry	46
	4.4.2 Geometries Utilised for Rotational Rheometry	47
	4.4.3 Parallel Plate Geometry	48
4.5	Rheometer	50
5.0	THIXOTROPIC STUDIES	52
5.1	Results and Discussion	52
	5.1.1 constant shear rate test	52
	5.1.2 Viscosity of Mixture of Silver Flakes with Silver Nano- powder	56
	5.1.3 Results from Hysteresis Loop Test	60
6.0	CREEP-RECOVERY AND OSCILLATORY SHEAR FLOW STUDIES	66
6.1	Results and Discussion	66
	6.1.1 Creep Recovery test	66
	6.1.2 Results from the Oscillatory shear test	73
	6.1.3 Correlation of oscillatory stress results to the ICAs structure	78
	6.1.4 Correlation of phase angle to quality of pastes formulation	82

7.0	CONCLUSION AND FURTHER WORK	84
7.1	Introduction	84
7.2	Conclusion	84
	7.2.1 Study the thixotropic behaviour of ICAs	84
	7.2.2 Study on the creep-recovery behaviour of ICAs	85
	7.2.3 Study of oscillatory shear flow of ICAs	86
7.3	Future work	87
	REFERENCES	88

LIST OF TABLES

Table		Page
4.1	ICAs formulation with silver flakes	42
4.2	ICAs formulations with silver flakes and silver nano-powder	43
6.1	Compliance data for silver flakes	69
6.2	Deformation and recovery index for silver flakes ICAs paste from creep recovery results	70
6.3	Compliance data for mixture of silver flakes and nano silver powder	71
6.4	Deformation and recovery index for mixture of silver flakes and nano silver powder	72
6.5	Oscillatory amplitude sweep parameter within the linear visco-elastic region for silver flakes	80

6.6	Oscillatory amplitude sweep parameter within the linear visco-elastic region for mixture of silver flakes and nano silver powder	80
6.7	Phase angle of silver flakes ICAs paste	82
6.8	Phase angle of mixture of silver flakes and nano silver powder ICAs paste	82

LIST OF FIGURES

Figures		Page
2.1	Reverse hysteresis loops for cement pastes tested using prolong cycle times	15
3.1	Schematic illustration of Newtonian fluids flow	21
3.2	Flow curve of a Newtonian fluid	23
3.3	Flow curve for a pseudoplastic fluid	25
3.4	Viscosity as function of shear rate for a dense suspension, (a) upper Newtonian region, (b) shear thinning region, (c) lower Newtonian region	25
3.5	Flow curve for yield stress fluids	28
3.6	Breakdown of thixotropic structure	32
3.7	Hysteresis loop obtained when shear rate is increased and decreased	33
3.8	Applied oscillatory stress and resulting strain for a visco-elastic material and an ideal solid	35

3.9	Schematic of creep-recovery response profile from a visco-elastic material	37
4.1	SEM Microstructure of (a) Silver powders and (b) Silver flakes	44
4.2	EDAX pattern for silver (Ag)	45
4.3	Couette flow in the parallel plate geometries	47
4.4	Parallel-plate geometry	48
4.5	Physica MCR301 rheometer	51
4.6	Parallel Plate of Physica MCR301 rheometer	51
5.1	Effect of Constant Shear on Paste A	54
5.2	Effect of Constant Shear on Paste B	54
5.3	Effect of Constant Shear on Paste C	55
5.4	Effect of Constant Shear on Paste D	55
5.5	Constant shear rate for Paste A and Paste E	57

5.6	Constant shear rate for Paste B and Paste F	58
5.7	Constant shear rate for Paste C and Paste G	59
5.8	Constant shear rate for Paste D and Paste H	60
5.9	Hysteresis flow curve of Paste A and E	61
5.10	Hysteresis flow curve of Paste B and F	62
5.11	Hysteresis flow curve of Paste C and G	63
5.12	Hysteresis flow curve of Paste D and H	64
5.13	Recovery Index for Paste A to Paste H	65
6.1	Creep recovery for silver flakes at 10 Pa	67
6.2	Creep recovery for mixture of silver flakes and silver nano-powder at 10 Pa	68
6.3	Compliance value of creep recovery graph	69
6.4	0.8wt% silver flakes	74

6.5	0.6wt% silver flakes	74
6.6	0.4wt% silver flakes	75
6.7	0.2wt% silver flakes	75
6.8	0.8wt% mixtures of silver flakes and nano silver powder	76
6.9	0.6wt% mixtures of silver flakes and nano silver powder	76
6.10	0.4wt% mixtures of silver flakes and nano silver powder	77
6.11	0.2wt% mixtures of silver flakes and nano silver powder	77
6.12	Stress where the $G'=G''$ for silver flakes	81
6.13	Stress where $G'=G''$ for mixture of silver flakes and nano silver powder	81

LIST OF ABBREVIATIONS

ICAs	Isotropic Conductive Adhesives
Ag	Silver
G'	Storage Modulus
G''	Loss Modulus
LVER	Linear Visco-elastic Region
PCB	Printed Circuit Board
DGEBA	Diglycidyl Ether of Bisphenol-A
Cu	Copper

Chapter 1

Introduction

1.1 Research Background

Due to the toxicity of lead in electronic products, legislation has been proposed to reduce the use of lead and even banning of lead from electronics. The two main directives are the European Union (EU) legislation 'Waste from Electronic and Electrical Equipment (WEEE) and 'Restriction of the use of hazardous substances in electrical and electronic equipment' (ROHS) directive that will ban the use of lead in new electronic products.

Solder paste are dense suspensions that exhibit complex flow behaviour under the influence of stress or strain. Solder pastes have been reported to possess thixotropic behaviour (Durairaj et al., 2004), shear thinning behaviour (Anderson et al., 1995) and exhibit a yield point during paste flow (Durairaj et al., 2008). Previous studies have confirmed that the viscosity of the solder pastes increases with greater metal contents, and decreases with increasing particle size distribution and temperature (Haslehurst, 1996). Several papers have attempted to correlate rheological measurement to printability (Bao et al., 1998, Durairaj et al., 2009) and slumping (Durairaj et al., 2002). Isotropic conductive adhesives (ICA's) have been considered as the most promising alternatives of lead-based solder due to their low processing temperature and environmental friendliness (Lu et al., 1999; Irfanand Kumar, 2008). The ICA's material consists of two components;

a polymer matrix and electrically conductive fillers. Previous studies on rheological characterization of ICA's were focused on correlating the rheological behavior to the printing performances (Durairaj et al., 2009; Durairaj et al., 2004). As the current trend for miniaturization is set to continue, formulation of isotropic conductive adhesives with various filler materials such as chemical modified silver flakes (Ho et al., 2013; Fan et al., 2011), new filler materials such as silver coated polymer spheres (Nguyen et al., 2013), mixture of silver nanoparticles (Li et al., 2011) have been focusing on achieving electrical and mechanical properties that are comparable to conventional silver flake-based isotropic conductive adhesives. The focus of rheology on this work has been attributed mainly to characterizing the viscosity of the new formulation. As these works have not provided an in-depth study of rheological properties of ICA's. The incorporation of filler materials into the polymer changes the rheological properties due to the different shapes and sizes, particle-matrix interactions and strong particle-particle attractions.

1.2 Problem Statement and Research Objectives

The development of new pastes (solder pastes and isotropic conductive adhesives) formulations is a very complex process because the paste rheology is known to be governed by a large number of parameters. These parameters typically include solder powder particle size, flux/vehicle medium, and volume fraction. In addition, the paste manufacturing industry has used viscosity as the key attribute for characterising the flow behaviour of pastes

materials. This attribute alone does not adequately describe why a paste prints differently under different conditions. With more extensive chemical and physical characterisation of the properties of paste it should be possible to understand why certain process parameters and environmental factors cause printing problem at ultra-fine pitch.

Hence, an understanding of the flow behaviour of the paste is important for achieving consistent paste deposit volume and reduction in the printing defects, ultimately increasing production yield. In particular, full characterisation of the visco-elastic properties of pastes is essential for determining the right printing process parameters, and ultimately for achieving proper control of the printing quality. The work reported in this thesis is concerned with the rheological characterisation of pastes designed for ultra fine pitch flips chip assembly and their application to the stencil printing process. This study on the rheological characterisation of isotropic conductive adhesives (ICAs) has three main objectives, as follows:

1. To study the effect of constant shear and hysteresis shear on the thixotropic behaviour of silver (Ag) based ICAs pastes
2. To study the paste creep deformation and recovery behaviour of silver (Ag) based ICAs pastes
3. To study the solid-like and liquid-like oscillatory shear flow behaviour of silver (Ag) based ICAs pastes

1.3 Overview

Chapter 1 presents the introduction to the study, the aim and the objectives of the work, and also provides an overview of the thesis.

Chapter 2 provides the results of the literature review on rheology of pastes, linear visco-elasticity and thixotropic behaviour of the suspensions. The chapter gives a review of the previous reported work on the behaviour of suspensions.

Chapter 3 gives an overview of the basic and fundamentals concepts about the rheology study. This chapter concerns about the basic definition of rheology, the basic parameters used in rheology such as; viscosity, shear rate and shear stress, it also introduces the various fluid systems like viscous and non-Newtonian fluids. This chapter also present the concept of the linear visco-elasticity and the thixotropic behaviour of the fluid.

Chapter 4 presents a description of the materials used, experimental equipment and parameters used for different parts of the study. The variation of rheology and weight fraction of ICAs with three types of fillers is investigated.

Chapter 5 presents the study of thixotropic behaviour of the paste samples, which described by using the constant shear and hysteresis flow curve. The chapter 6 is the study of creep-recover and viscoelasticity of the sample pastes by using oscillatory stress experiment.

The final chapter, chapter 7 presents the summary of the study, the main conclusions from the study and the suggestions for the further work.

CHAPTER 2

LITERATURE REVIEW

2.1 Introduction

This chapter presents the relevant literature review on the rheological characterisation of solder pastes and ICAs used as the interconnection material in the assembly of electronic devices. The chapter is consisted of two main sections; the first section gives a review of previous studies on rheology of solder pastes and ICAs. In this section, a general literature search was carried out to identify the previous work on the rheology of solder pastes and ICAs. Based on the literature review, two main areas were identified; firstly the visco-elastic behaviour of the pastes and secondly the thixotropic behaviour of the paste materials. In addition, it is hoped that the two areas mentioned above will allow for a better understanding of the rheological test methods that can be used in characterising the rheology of the pastes.

The second section deals with the detailed review of previous work on visco-elastic behaviour of suspensions and the thixotropic behaviour of paste material. The aim of these sections is to identify the approach to be used for visco-elastic behaviour and thixotropic behaviour in suspensions.

2.2 Rheology of Pastes

Extensive work was carried out on the factors that contributed to the viscosity of solder pastes. They identified factors such as particle size distribution and shape, metal content, temperature, and flux/vehicle systems as those that affect the rheology of solder pastes. Study by Jirinec (1984) reviewed the role of the solder powder, particle size, shape and distribution, and their effect on paste performance.

They discussed and covered areas such as solder paste composition, solder powder particle size distribution, metal content and its effect on viscosity and screenability of the paste. These two studies were the earliest attempts to understand the extent to which the paste composition affects its rheology and processing performance.

In the early 1990s, a series of studies were conducted with the primary aim of correlating the rheology of pastes to the pastes stencil printing performance. Ogata (1991) carried out one of the earliest studies to determine the relationship between the rheology and printability of solder paste based on its thixotropic index. Unfortunately, Ogata did not provide details of the viscometer, the particle size distribution or flux/vehicle type of the six different solder pastes evaluated. This lack of detail study made it impossible to compare this result with other studies or reproduce the results.

In another study, Carpenter et al. (1994) also attempted to correlate the rheology of solder paste to the paste printing performance. A viscosity and yield stress test were carried out to study the rheological properties of different solder pastes. Their results showed that pastes with high viscosity did not

slump but printed poorly and that skipping defects was observed for high viscosity paste. The study also found that a very solid-like solder paste required the application of a higher printing pressure and also exhibited a poor aperture withdrawal characteristic.

Lapasinet al. (1994) reported a study on the rheology of solder paste using three different rheological test methods, the constant shear rate test, high shear rate followed by low shear rate and hysteresis loop test. In all three tests the focus was to measure a single parameter, which is the viscosity of the paste. It was found that hysteresis test provided a good measure for differentiating between solder pastes. It was claimed that the viscosity alone is sufficient for making reliable prediction of the flow behaviour of solder pastes.

In a study by Anderson et al. (1995), they raised the interesting point about the repeatability and reproducibility of the viscosity measurements. The study showed that viscosity is very difficult to measure due to the wall slip phenomena in the printing of the pastes. It was suggested that the apparent viscosity is not the measure of the true viscosity of solder paste. In order to eliminate slip, sandpaper was attached to the upper plate (interior side) to prevent slipping, which delayed the slip formation but did not prevent it. Although the slippage was observed, the author did not attempt to correct the viscosity data or attempt to use some form of visualisation technique to understand the slip formation in the pastes.

Many of the previous studies therefore did not investigate the impact of the visco-elastic property of solder pastes. Rather the main focus of these studies was to determine the printing behaviour of pastes using single point viscosity measurements. In addition to focusing on the viscosity measurement,

many of the previous studies did not give sufficient information on the experimental procedures used for characterising the rheology of solder pastes. Consequently, it was very difficult to reproduce these results from the previous studies.

Towards the end of 1990s, the focus shifted from basic viscosity measurement to investigating the visco-elastic behaviour of the pastes, for example, Lapasinet al. (1998) studied the visco-elastic behaviour of solder paste using both the oscillatory and creep/recovery test. One of the finding of this study is that the contribution of the disperse (Lapasin et al. 1998) phase is almost negligible at low shear or frequency despite the high content of the disperse phase, and increases with increasing strain rate or frequency, essentially concerning only the viscous properties of the paste. This means that adjusting the formulation of the flux vehicle can properly modulate the rheological properties of the paste.

Another study by Baoet al. (1998), investigated the visco-elastic properties of solder pastes, but there was no attempt to determine the linear region of solder paste and flux/vehicle system. The study speculated that the linear visco-elastic region could be below 40Pa. In yet another study, Ekereet al. (1998), studied the effect of high frequency oscillatory shear on solder paste. One of the conclusions from the study is that the dynamic viscosity of the samples decreased with increasing frequency. The implication of this finding is that solder paste will exhibit fluid like behaviour at higher stresses and frequencies, which can facilitate the aperture filling process during stencil printing.

In separate studies, Baoet al. (1998) and Ngutyet al. (1999) used the

creep-recovery test to predict the conditions for the onset of slump behaviour in solder paste. Both studies used the creep-recovery index for classifying the slump tendency in different pastes. These early reports on work on the visco-elastic behaviour of pastes identified the need for more information on the solid and liquid characteristics of the pastes, especially the need for further work on the linear visco-elastic region of pastes. For example, Nguty et al (1999) did not indicate if the applied stress used in the creep-recovery test was within the linear visco-elastic region.

Unfortunately, none of the previous studies address the issues of the methodology for the determination of the linear visco-elastic region. The determination of the linear visco-elastic region is very important, as it is the basis for studying visco-elastic behaviour (solid and liquid characteristic) of solder paste. In addition to the solid and liquid characteristics, the applied stress in the creep-recovery test must be within the linear visco-elastic region. Details of the study on the use of the oscillatory test method for studying the visco-elastic behaviour of solder pastes and ICA is presented in chapter 6.

The introduction of Pb-free soldering is being driven by a European directive, on reduction of Waste from Electronic and Electrical Equipment (WEEE), which calls for the elimination of lead containing materials from electronics products by June 2006. This has put tremendous pressure on the electronics industry to find a suitable replacement for the widely used tin/lead based solder alloy. One material that is already being evaluated is the tin/silver/copper alloy. The transition from lead to lead-free solder pastes will require investigation of the rheological properties of lead-free solder pastes.

In one study by Nguty et al. (2000), the rheological properties and the

printing performance of lead-free solder pastes was evaluated. In their study, various rheological properties were measured to compare lead and lead-free pastes, and it was found that the lead and lead-free solder pastes have similar rheological properties. However, they did not include any visco-elastic measurements in this study. In yet another study, Nguty et al. (2000) compared the rheological properties of solder and solar pastes under steady shear and creep-recovery. The creep-recovery test was used to predict the onset of slump behaviour in pastes, as slumping is one of the main printing defects faced by the surface mount assembly process. Unfortunately, this study did not address the visco-elastic behaviour of the paste in more details.

Apart from studies conducted on the evaluation of the rheological properties of paste and their printing performance, the viscosity of pastes as a function of temperature was also studied by Mindel et al. (1991) and Nguty et al. (2000).

Mindel et al. (1991) measured the viscosity of solder pastes both at different temperatures, namely: 25⁰C, 50⁰C and 75⁰C. Unfortunately, Mindel did not provide the details of the experiments, for example, there was no information on flux medium, the paste particle size or the plate geometries on the rheometer used in the study. In the other study, Nguty et al (2000) investigated the effect of temperature on the rheology of solder pastes. Unlike Mindel (1991), the report provided more details of the experimental work. However, the temperature range investigated by Mindel and Nguty is not representative of those used in industry as the reflow temperatures for solder pastes are very usually above 75⁰C.

Another important issue in the challenge of developing lead-free solder

paste is the shelf life of solder pastes. This is because exposing the paste for long periods on the shelf may lead to separation between the flux and particles which ultimately may have adversely impacted the rheological properties of the solder paste. In their study, Ngutyet al. (2000) monitored the change in viscosity of solder paste stored at room temperature over a period of 5 months, and the results showed 60% increase in the viscosity for samples kept at room temperature. In addition, the study by Nguty et al. (2000) also provides a good background of solder paste materials (e.g. constituent of solder paste, solder powder and metal alloy and flux/vehicle medium). In a more recent work, Jackson et al. (2002) evaluated the visco-elastic behaviour of specific lead-free solder pastes including SnAgCu solder paste.

In their study, Jackson et al. (2002) performed oscillatory test measurement on various lead-free solder pastes and flux systems. One of the findings of the study is that the flux vehicle system has a direct effect on the flow behaviour of the solder pastes. However, one of the limitations of this study is that there was no attempt to determine of the linear visco-elastic region of the pastes being studied.

2.3 Visco-elastic and Thixotropic Behaviour in Paste Suspensions.

Based on the literature search on solder paste, three main areas were identified; visco-elastic behaviour and thixotropic behaviour of pastes.

2.3.1 Visco-elastic Behaviour of Paste Suspensions

As stated in the previous section, there are relatively few studies reported in the literature on the impact of visco-elastic behaviour of pastes (solder paste and ICA). Most of the earlier work review on solder paste has focused on using viscosity as the only parameter to characterise the flow behaviour of the pastes. The work reviewed in this section is that related to visco-elastic behaviour of suspensions.

Phan-Thien et al. (1998) investigated the linear visco-elastic properties of flour-water doughs at different water concentrations. The results from the strain sweep experiments showed that the linear visco-elastic strain limit is extremely low. In another study conducted by Berli et al. (2000), they investigated the solid to liquid transition of microgel suspensions through oscillatory stress sweep. In another study, Ghezzehei et al. (2001) investigated the rheological properties of wet soils and clays under oscillatory stress test.

In another study, Amoros et al. (2001) studied the visco-elastic behaviour of clay suspensions through small amplitude oscillatory tests. The study shows that adding quartz to a colloidal suspension, it raises the value of the elastic component G' , as well as the viscous component G'' . For the studied system, at moderate quartz contents additions, the G''/G' ratio, which is directly related to the material's visco-elastic behaviour, depends almost exclusively on the deflocculation state of the clay suspension.

Heymann et al. (2002) studied the solid-liquid transition of highly concentrated suspensions in oscillatory amplitude sweeps. The non-linear behaviour of medium and highly concentrated suspensions of spherical quasi-

monodisperse particles with two different sizes was studied using controlled shear stress (CSS) amplitude sweeps of an oscillatory shear flow. The influence of the sample preparation, the mode of the experiment and the parameters of the amplitude sweep such as logarithmic ramp time, measurement time and frequency were investigated. The study found that the logarithmic ramp time and the measurement time influenced the experiment results at low shear stress amplitudes.

In another study, Bekkour et al. (2002) investigated the linear visco-elastic behaviour of Bentonite-water suspensions. Creep and oscillatory shear experiments in the linear visco-elastic domain were carried out on the bentonite-water suspensions at different solid fractions. It was found that bentonite dispersions exhibit important visco-elastic behaviour which could be represented by the generalized Kelvin-Voigt mechanical model.

In one study, Wildmoser et al. (2004) evaluated the microstructure and quality characteristics of ice cream through oscillatory measurement technique. In a rotational rheometer (plate-plate geometry) the rheological behaviour of ice cream was studied by performing oscillatory measurements at low deformation amplitudes for three different temperature ranges corresponding to important consumer properties of ice cream. The study correlated the oscillatory test parameters to the ice crystal microstructure, determined the rigidity and "scoopability" of ice cream at low temperatures (-20°C to -10°C).

2.3.2 Thixotropic Behaviour in Paste Suspensions

Since the late 1950's several experimental techniques have been developed for measuring the thixotropy of suspensions. Ish-Shalom et al. (1960) used the hysteresis loop test to measure the thixotropic behaviour of cement pastes. In the hysteresis loop test, the material is subject to increasing shear rate or stress to a pre set maximum shear rate/stress value. The shear stress/rate is then decreased to a preset minimum value. The 'area' enclosed by the flow curve gives a measure of the thixotropic behaviour of the material. They showed that the 'area' enclosed between the up curve and down curves (i.e. hysteresis) is a measure of the degree of thixotropy in the samples.

Mewis (1979) presented a review of the time-dependent behaviour associated with thixotropy on various suspensions. Mewis also traced the evolution of the term thixotropy and provided a generalised definition. In the review, various experimental methods, such as hysteresis loop and constant shear rate test, which are relevant in the study for the thixotropic behaviour of suspensions, were discussed.

In another study, Roy and Asaga (1979) also investigated the thixotropic behaviour of cement paste. The hysteresis loop tests were performed on the cement paste. They observed that the down curve is higher than the up curve, often resulting in a formation of 'Figure 8' response shown in Figure 2.1. The formation of 'Figure 8' curve in the hysteresis loop test is known as reverse hysteresis. In another study by Banfill et al. (1981) on cement paste they also observed the reverse hysteresis loop curve behaviour

and suggested it could be due to stiffening of the paste.

The study by Tattersall and Banfill (1983) suggested that the experimental approach to characterise the thixotropic behaviour in a material can be classified into two main test methods; (i) hysteresis loop test and (ii) steady state/equilibrium test. Lapasinet al. (1983) and Cauffinet al. (1984) utilised a steady state approach to study the flow behaviour of cement pastes. At a given shear rate, viscosity is measured until equilibrium is obtained. The equilibrium viscosity value represents the minimum viscosity that can be obtained for a given shear rate. The study showed that the time to reach equilibrium viscosity is on the order of 8 to 15 minutes. The authors used the difference between the peak viscosity and equilibrium viscosity as the measure of the thixotropy of the material.

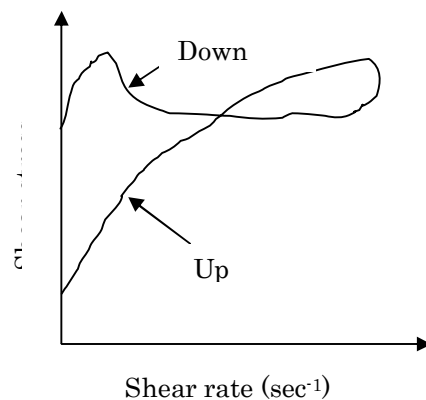


Figure 2.1: Reverse hysteresis loops for cement pastes tested using prolonged cycle times (Adapted from Banfill and Saunders, 1981)

Ramaswamy et al. (1992) studied the time dependent stress decay rheology of stirred yogurt. Two stirred yogurts were subjected to various shear

rate between $100\text{-}500\text{s}^{-1}$ and temperatures of $10\text{-}25^{\circ}\text{C}$. The study used the equilibrium shear stress method to characterise the time dependent behaviour (thixotropy) of the yogurt. The study found that equilibrium shear stress was not reached even after 60 seconds.

Usui (1995) developed a thixotropy model to study the complex rheological behaviour of coal-water mixtures. The idea of this model is based on the assumption that the thixotropic behavior of dispersed systems is well described by the coagulation process of the minimum sized particles contained in a dispersion system and the break-up process of coagulated clusters. But the study did not mention the applicability of the model to other suspensions.

Perretet al. (1996) studied the thixotropic behaviour of fine-grained mud from Eastern Canada. Just like the previous work, the author used the hysteresis loop test to characterise the thixotropic behaviour of the mud. In this work, they measured the areas within the hysteresis loop developed, which was used as an indicator of the thixotropic behaviour of the pastes. They also showed that the hysteresis loop area can be related to the volume of the sample sheared in a time unit. From the literature review, it seems that the hysteresis loop test is pre-dominantly used to determine the thixotropic nature of a suspension.

However, Barnes (1997) in a review paper on the subject of thixotropic behaviour raised few points relating to the use of hysteresis loop test. According to Barnes, the hysteresis loop test is a quick way of measuring thixotropic behaviour of a suspensions but the test may not represent the actual structural breakdown and build-up that is occurring in the suspensions itself. Furthermore, the down curve in the hysteresis loop may be influenced by wall

slip. This may result in an error in the measurement of the thixotropic behaviour of the suspensions.

In another study, Pignonet al. (1998) investigated the thixotropic behaviour of a colloidal dispersion of clay consisting of disk-shaped particles by means of a combination of rheometric measurements, static light scattering, and small-angle neutron scattering. The study found that at rest, the structure of the gel consists of dense micrometer-sized aggregates. Under shear, in the case of volume fractions with ($1 \leq D \leq 1.2$), a butterfly-type light scattering pattern is observed. This is attributed to the formation of rollers within the dispersion, which align themselves on average perpendicular to the direction of shearing. This produces an increase in the resistance to flow. Under shear flow conditions, the fall in viscosity is due to orientation and disaggregation processes occurring at length scales of the order of $1 \mu\text{m}$.

Phuapradit et al. (2002) investigated the critical processing factors, which could affect the rheological behaviour of the wax-based vehicle. The vehicle in a gel region behaved thixotropic in nature, as indicated by a hysteresis loop. The results of this study indicated that shear rate and cooling rate are the critical processing factors in controlling the viscosity of the final product and must be well controlled in the manufacturing procedure.

Chapter 3

RHEOLOGY

3.1 Rheology

Rheology is the study of the flow and deformation of matters. It includes classical fluid mechanics and elasticity, which covers a broad range of materials like Newtonian liquids (such as water) and hard solids (such as wood and steel). Professor Bingham coined the term “rheology” in 1929 and from then on there has been a rapid development of the subject. Rheology is also used to describe the flow and deformation of complex materials such as rubber, molten plastics, polymer solutions, slurries and pastes, electro-rheological fluids, blood, muscle, composites, soils, and paints.

A material can be classified as either a Hookean solid, a Newtonian liquid or as visco-elastic. In perfect Hookean elastic solid, the material deforms when a force is applied and it relaxes (reverses) on the removal of the force. The deformation energy is stored and is subsequently recovered on relaxation. In Newtonian viscous fluids, the deformation causes flow, which ceases on the removal of the force, and the energy, is dissipated as heat.

The vast majority of fluids exhibit a rheological behaviour that classifies them in a region somewhere between the liquids (viscous) and the solids (elastic), for example, the toothpaste that sits apparently motionless (elastic behaviour) on the bristles of the toothbrush can be easily squeezed (viscous behaviour) from the tube. As a result, the materials, which exhibit

elastic and viscous properties simultaneously, are called visco-elastic materials. These materials may be either visco-elastic solids (i.e. elastic solids which, during deformation, exhibit some viscous effects due to energy dissipation) or viscous fluids (i.e. viscous fluids which exhibit some elastic behaviour). If a wide range of stress is applied over a very wide spectrum of time, then it is possible to observe liquid-like behaviour in some solids, and solid-like behaviour in some liquids..

3.2 Basic terms associated with Rheology

3.2.1 Viscosity

Viscosity is a measure of the resistance of a fluid to deformation under shear stress, as this is commonly perceived as "thickness", or resistance to pouring. Viscosity can also be described as a fluid's internal resistance to flow and may be thought of as a measure of fluid friction (Barnes, 2000). Thus, water is "thin" because of having a low viscosity, while vegetable oil is "thick" due to having a high viscosity. Viscosity can be measured with a viscometer or a rheometer, typically at 25°C (standard state). For most Newtonian fluids the viscosity remains constant over a wide range of shear rates. The fluids, which exhibit a variable range of viscosity values, are referred to as non-Newtonian fluids.

In general, in any flow, the liquid layers move at different velocities and the fluid's "thickness" arises from the shear stress between these layers that ultimately opposes any applied force, see Figure 3.1. As can be seen in

Figure 3.1, the friction between the fluid and the moving boundaries cause the fluid to shear and the force required for this action is a measure of the fluid's viscosity. Isaac Newton postulated that, for straight, parallel and uniform flow, the applied shear stress, τ , between the liquid layers is proportional to the velocity gradient, $\partial u/\partial y$, as given in Equation 3.1 (Barnes, 2000).

$$\tau = \mu \frac{\partial u}{\partial y} \quad (3.1)$$

In Equation 3.1, the constant μ is known as the *coefficient of viscosity*, *viscosity*, or *dynamic viscosity*. As was stated earlier, many fluids, such as water and most gases, satisfy Newton's criterion and are known as Newtonian fluids. But non-Newtonian fluids exhibit a more complicated relationship between shear stress and velocity gradient than simple linearity. In industrially important situations non-Newtonian fluids may exhibit very complicated rheological behaviour, but from the pragmatic point of view the decisive property of the fluid flow behaviour is often its variable viscosity with changes in shear rate. The simplest approach in the case discussed above is a generalization of Newton's viscosity Equation (3.1) in the following form:

$$\tau = \eta \dot{\gamma} \quad (3.2)$$

Where τ = shear stress, η = viscosity and $\dot{\gamma}$ = shear rate. The SI unit of dynamic viscosity is the pascal-second (Pa·s), which is identical to 1 N·s/m² or 1 kg/(m·s).

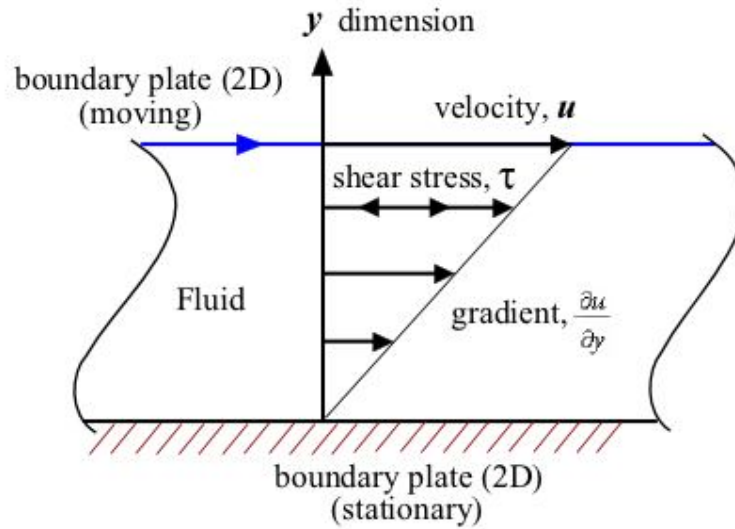


Figure 3.1: Schematic illustration of Newtonian fluids flow

3.2.2 Shear Rate

Examination of the schematic diagram in Figure 3.1 shows that the shear stress, τ , causes the liquid to flow in a special laminar flow pattern. The maximum flow speed, u_{\max} is found at the upper boundary and the speed drops across the gap size, y down to $u_{\min} = 0$ at the lowest boundary (in contact with the stationary plate). Laminar flow means that infinitesimally thin liquid layers slide on top of each other, similar to the card in a deck of cards. One laminar layer is displaced with respect to the adjacent ones by a fraction of the total displacement encountered in the liquid between both plates. The velocity gradient across the gap size is named “shear rate”, and in its general form it is

mathematically defined by a differential. The velocity gradient, $\frac{\partial u}{\partial y}$ for any section of the liquid between the plates is constant and it is equal to $\frac{u}{y}$.

The shear rate shown in Equation 3.3 is expressed in unit reciprocal seconds (sec^{-1}).

$$\dot{\gamma} = \frac{du}{dy} = \frac{u(\text{velocity})}{y(\text{thickness})} \quad (3.3)$$

3.2.3 Shear Stress

If a force (F) is applied to an area (A), which is at the interface between the upper plate and the liquid underneath, it will lead to a flow in the liquid layer. This force per unit area is called the shear stress, τ , with a unit of Pascal (Pa), shown in Equation (3.4).

$$\tau = \frac{F(\text{force})}{A(\text{area})} \quad (3.4)$$

3.3 Viscous Fluids

3.3.1 Newtonian Fluids

The simplest relationship between shear stress and shear rate for a fluid is one that is constant or directly proportional, as given by the Equation (3.5).

$$\tau = \eta \dot{\gamma} \quad (3.5)$$

From the Equation 3.5, the symbol η , is referred to as the Newtonian

viscosity, and the flow curve (a plot of shear stress versus shear rate) is therefore a straight line passing through the origin, as can be seen Figure 3.2.

Newtonian behaviour is rarely observed in suspensions (except in those non-interacting particles, which are fully dispersed – light concentrations in which particle collision rarely occurs). The paste materials used in the studies reported in this work is dense suspensions, exhibiting very densely packed particles which are in close contact with continuous interactions between particles – these pastes therefore exhibit non-Newtonian flow behaviour.

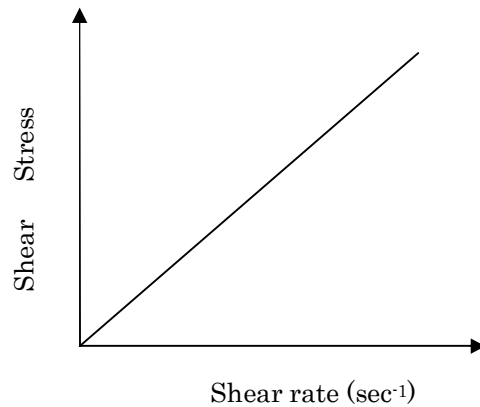


Figure 3.2: Flow curve of a Newtonian fluid

3.3.2 Non-Newtonian Fluids

As stated earlier in section 3.2.1, non-Newtonian fluid is one that does not exhibit a linear relationship between shear stress and shear rate. Non-Newtonian fluids can be classified into three main categories; (i) Pseudoplastic, (ii) Shear thickening and (iii) Yield stress.

3.3.2.1 Pseudoplastic

Pseudoplastic fluids are typically suspensions of solids or long chain polymer strands in a liquid medium. As the shear rate increases, the structure of the fluid becomes more orderly, which steadily reduces the apparent viscosity, see Figure 3.3. The power-law model also referred to as Ostwald-de Waale model (Ostwald 1926), Equation (3.6), may be used to model the reological behaviour of pseudoplastic fluids.

$$\tau = k\dot{\gamma}^n \quad (3.6)$$

where the parameter k is defined as the pre-exponential factor or consistency index and n as the exponential factor or the flow behaviour index. The value of constant k gives an indication of the viscous behaviour of the fluid, while the value of the index n describes the extent of the deviation of the fluid behaviour from Newtonian behaviour. For pseudoplastic fluids n must be less than unity. If n is equal to one, then equation (3.6) reduces to the Newtonian model, equation (3.5) and k becomes the Newtonian viscosity, μ . When n is greater than one the fluid is said to exhibit a shear thickening behaviour, which is explained in section 3.3.2.2. In reality however, most pseudoplastic fluids cannot be described by the power law model over a wide range of shear rates, as there is typically a region of Newtonian behaviour at very low shear rate and a second Newtonian region at very high shear rates, see Figure 3.4 (Ferguson et al. 1991).

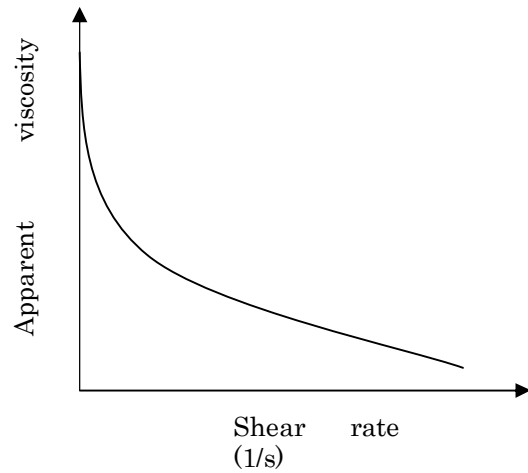


Figure 3.3: Flow curve for a pseudoplastic fluid

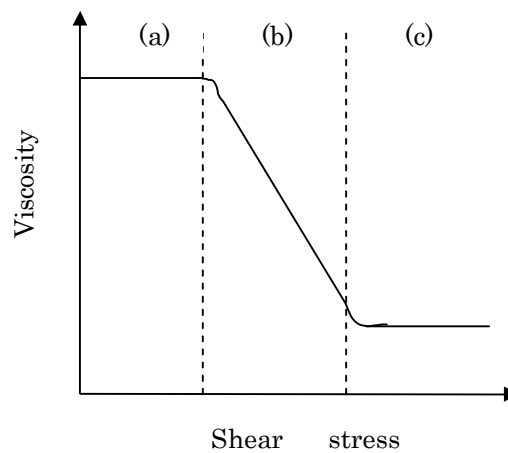


Figure 3.4: Viscosity as function of shear rate for a dense suspension, (a) upper Newtonian region, (b) shear thinning region, (c) lower Newtonian region

More complex models based on the power-law model have been proposed to improve the description of pseudoplastic fluid behaviour over a wide range of shear rates. The Cross model, Equation (3.7) incorporates two terms η_0 and η_∞ , which corresponds to the constant viscosity regions at very low and very high shear rates respectively (Cross, 1965). The index m and

constant k are the dimensionless constants associated with the breakdown of the structure. The degree of shear thinning is dictated by the value of m (where m tending towards unity represents shear thinning liquid while m tending towards zero represents Newtonian liquids).

$$\frac{\eta - \eta_{\infty}}{\eta_0 - \eta_{\infty}} = \frac{1}{1 + (k \dot{\gamma})^m} \quad (3.7)$$

3.3.2.2 Shear Thickening

Shear thickening behaviour should not be confused with dilatancy, which is a change in volume on deformation, though dilatancy is often used to describe shear thickening behaviour. Suspensions of solid in liquid are often capable of shear thickening behaviour over certain ranges of shear rate. The degree of shear thickening and its onsets is a function of the solids concentration, the particle shape and size distribution. At rest the particles are assumed to be situated in such a way that the void space between particles is at a minimum, but as the shear rate increases the particles becomes more disordered and there may be insufficient liquid to fill the space between the particles leading to direct particle-to-particle contact which causes an increase in the apparent viscosity of fluid or shear thickening behaviour (Kevra, 1989).

In practice, it is extremely rare for a fluid to exhibit a pure shear thickening behaviour. Provided that the pre-exponential parameter n , given in Equation 3.7 is greater than one, the rheological models presented for shear-thinning fluids can also be used to describe the behaviour of the shear thickening fluid. In some practical applications shear thickening behaviour

may be observed over a particular range of shear rate values and in these cases a number of rheological models can be used to describe the fluids behaviour in these shear rates regime (Akroyd, 2004).

3.3.2.3 Yield Stress Behaviour

The yield stress of a fluid is commonly defined as the stress that is required to initiate flow of the material. Some of the more simple types of flow curves associated with yields stress behaviour in fluids are presented in Figure 3.5. The yield stress, however, is not easily measured and values of the yield stress for a fluid will often vary depending on the measurement technique (Steffe, 1992). It is believed that the response of a fluid material is very similar to that exhibited by an elastic solid, but the response changes once the yield stress is reached – at which point the fluid begin to exhibit a flow behaviour. The yield stress behaviour is usually explained by the fact that the fluid contains an internal structure that is able to resist a certain amount of stress before flow commences. There is some discrepancy in the literature as to the true nature of the yield stress and whether or not it truly exists (Barnes and Walters, 1985). If the yield stress does indeed exist then the variable nature in measured values of yield stress suggest that there may be multiple types of structures involved that have varying level of significance during different type of test (Cheng, 1986). The two most common types of test to determine the yield stress are direct measurement and extrapolation. Numerous methods have been proposed for the direct determination of the yield stress, but one of the more simple methods uses a generic rotational

rheometer and vane geometry (Nguyen and Boger, 1985). In the case of a single point viscometer, a direct measurement of the yield stress may not be possible. As a result of this, an extrapolation procedure must be used to obtain an estimated value for the yield stress. This means creating a tangent line at the end of the known data and extending it beyond that limit (until it reaches the y-axis). The stress value at the point of intersection of the tangent line to the y-axis is the yield stress value. A linear extrapolation can be easily done with a ruler on a written graph or with a computer (Akroyd, 2004).

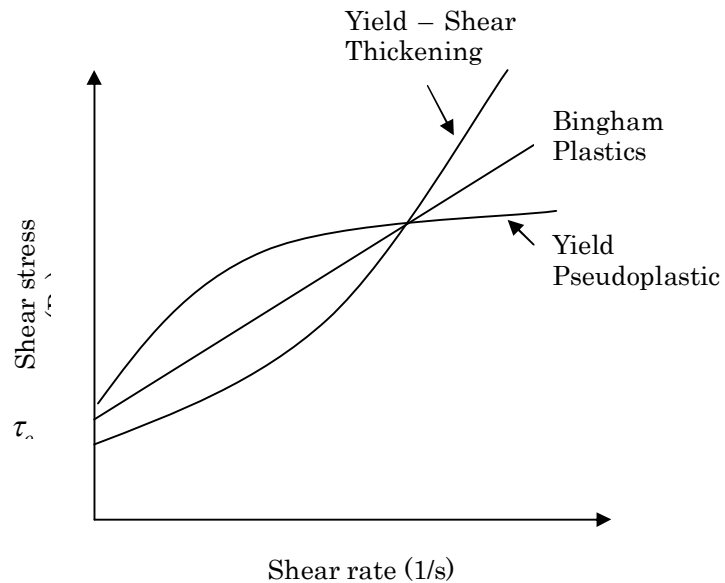


Figure 3.5: Flow curve for yield stress fluids

(a) Bingham Plastic Model

The simplest type of yield stress fluid model is the Bingham plastic model (Bingham 1922), shown in Equation (3.8). For this model once the yield stress is exceeded it is assumed that the fluid behaves like a Newtonian

fluid, where the shear stress increases proportionally with increases in shear rate. However, there are few suspensions and slurries for which the Bingham model can be used to describe the rheological behaviour over a wide range of shear rates. But over a small range of low values of shear rate the Bingham model may be more applicable for a wider range of suspensions.

$$\tau = \tau_y + \mu \dot{\gamma} \quad (3.8)$$

where τ_y is the yield stress (Pa), μ is the Newtonian viscosity (Pa.s) and $\dot{\gamma}$ is the shear rate (sec^{-1}).

(b) Yield Pseudoplastic Fluids

Generally most suspensions can be described as yield-pseudoplastic fluids; once the yield stress is exceeded the fluid can be expected to act similar to a non-yield stress shear thinning fluid (described previously in section 3.3.2.1). Two of the more simple models that exist for describing yield pseudoplastic fluids are Casson and Herschel-Bulkley model (Akroyd, 2004). Initially developed to describe the properties of printing inks but later shown to be suitable for some yield stress fluids, the Casson model is shown in Equation (3.9), (Casson, 1959).

$$\sqrt{\tau} = \sqrt{\tau_y} + \sqrt{\mu \dot{\gamma}} \quad (3.9)$$

The Herschel Bulkley model (Herschel and Bulkley 1926a, 1926b) studied rubber-benzene solutions and encountered non-linear behaviour, which they accounted for by proposing an empirical relationship containing three parameters, which is quite similar to the power-law model previously

described in section 3.3.2.1, with an additional yield stress term, τ_y , shown in equation (3.10). The Herschel-Bulkley model is more widely used than that Casson model because the extra term increases the range of fluid behaviour that can be described by the model.

$$\tau = \tau_y + A\dot{\gamma}^n \quad (3.10)$$

In both Casson and Herschel-Bulkley model, the fluid's yield stress can either be obtained from experimental measurement, such as the vane method (Nguyen and Boger 1985), or by extrapolation from measured rheological data such as the shear stress and shear rate, as previously explained in section 3.3.2.3.

(c) Yield Shear Thickening

Suspensions with particular properties of the solid particles and the suspending medium can exhibit yield shear thickening behaviour. In the case of yield shear thickening behaviour, the Herschel-Bulkley model, Equation (3.10), which was previously outlined for yield-pseudoplastic fluids can be used to describe the fluid rheological behaviour, except that pre-exponential parameter 'n' must be greater than one (Akroyd, 2004).

3.4 Thixotropy

All viscous fluids can exhibit thixotropy, because thixotropy reflects the finite time taken to move from any state of microstructure to another and

back again, as shown in Figure 3.6. Certain materials behave as solids under very small applied stresses but under greater stresses become liquids. When the stresses are removed the material settles back into its original consistency. This property is particularly associated with certain colloids which form gels when left to stand but which become sols when stirred or shaken, due to a redistribution of the solid phase (Barnes, 1997). Characterising the degree of thixotropy in pastes such as solder pastes and isotropic conductive adhesives is an important step in understanding the rheological behaviour of the material during stencil printing. The thixotropy effect is a result of aggregation of suspended particles and the attractive forces such as Van der Waals and repulsive forces due to steric and electrostatic effect on the particles cause the aggregation in the system. The repulsive force prevents the particles from approaching close to one another, and as a result, weak physical bonds hold the particles together. When no force is exerted on the suspension, the particle aggregation can form a spatial network, which creates an internal structure. When the suspension is sheared, these weak forces are broken, causing the network to break down into smaller aggregates. These aggregates can be broken down further into smaller flocs.

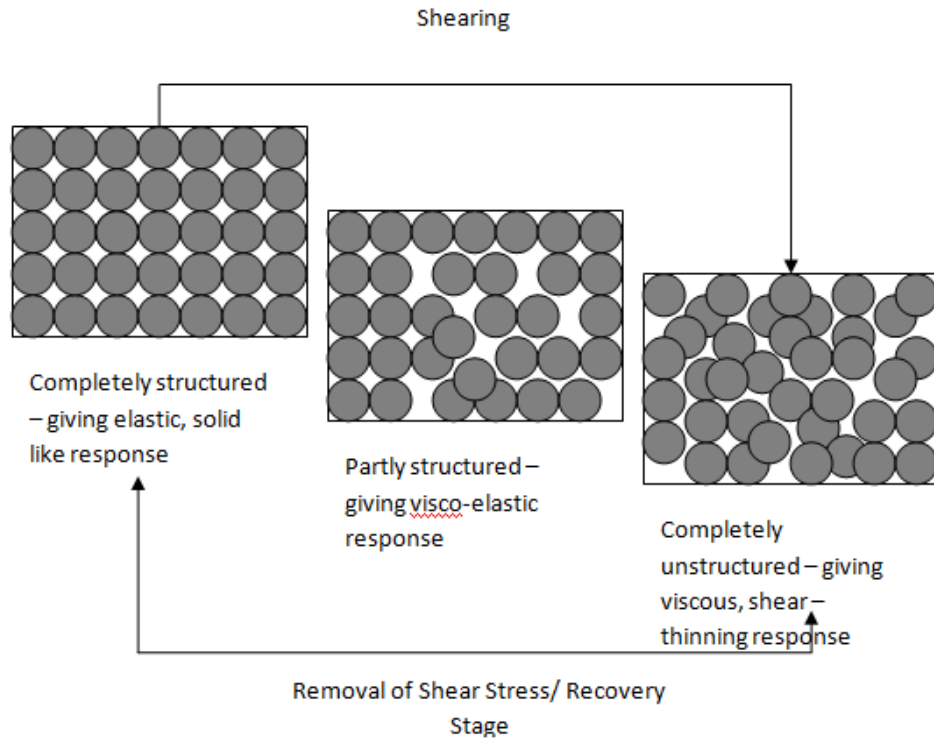


Figure 3.6: Breakdown of thixotropic structure

On the other hand, in less concentrated suspensions the Brownian motion and inflow collision can cause the formation of aggregates. Shearing or inflow collision can cause the particle to attach to other parts of the microstructure, which will increase the size of the aggregates. Besides shearing/inflow collision, Brownian motion can also cause an increase to the number of aggregates in the system. Brownian motion is the random thermal agitation of atoms and molecules, which cause them to move to a favourable position where they can, given the necessary attractive force, attach themselves to other parts of the microstructure (Barnes, 1997). After a period of time, at a given shear rate, a dynamic equilibrium is reached between the growth and destruction of aggregate.

Thixotropic materials can also exhibit shear-thinning behaviour. When

a thixotropic material is subject to increasing shear rates, the viscosity drops but when the shear rate is removed, the material structure recovers resulting in the hysteresis loop, shown in Figure 3.7. It should be noted that the rebuilding of the structure is not instantaneous upon the removal of stress. The area between the hysteresis loop is used as a measure of the ‘amount’ of thixotropy or the area enclosed within the loop can be used as an indication of energy required to break down the material structure.

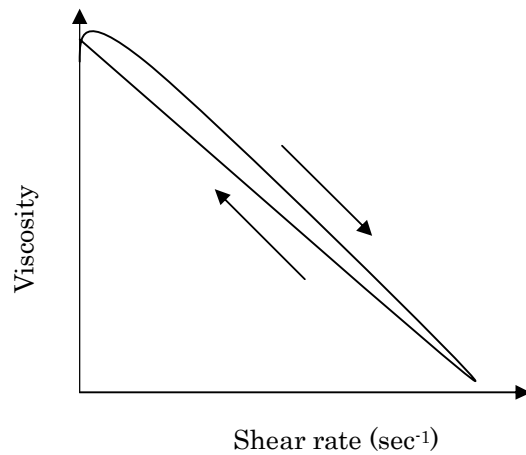


Figure 3.7: Hysteresis loop obtained when shear rate is increased and decreased.

3.5 Visco-elasticity

A good understanding of rheological properties and behaviour of paste is vital for establishing the condition for achieving good material processing performance. This is especially true when the material processing demands precise control of deformation and flow behaviour at various stages in the process. Most complex materials such as emulsion, dispersions, gels, pastes

and slurries exhibit visco-elastic behaviour during processing. For some processes the elastic behaviour is the dominant factor prohibiting higher production rates, while for other processes such as settling of fillers in a suspension with a continuous phase of high viscosity, the zero shear viscosity will be the governing factor. The visco-elastic flow behaviour can be characterised through oscillatory and creep-recovery test methods.

3.5.1 Oscillatory Test

Oscillatory test are typically used for studying the microstructure of complex emulsions, dispersions, gels, pastes and slurries. The oscillatory stress sweep is typically used to characterise the visco-elastic effect of complex materials. The oscillatory experiments can be designed to measure the linear or the non-linear visco-elastic properties of complex materials.

When applying a sinusoidal stress, the angular velocity (ω) and the stress amplitude (σ_o) are assigned parameters. The measured strain is therefore a sinusoidal function. The applied stress and the resultant strain are expressed as,

$$\sigma = \sigma_o \sin(\omega t) \quad (3.11)$$

$$\gamma = \gamma_o \sin(\omega t + \delta) \quad (3.12)$$

Where δ is the phase shift, $\omega=2\pi f$ where f is the frequency, and t is the time.

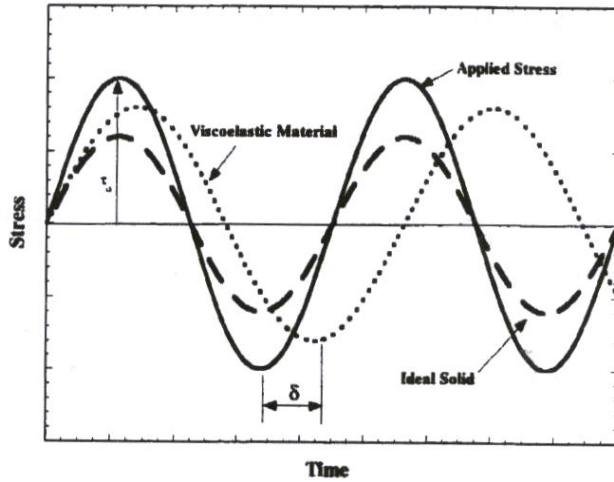


Figure 3.8: Applied oscillatory stress and resulting strain for a visco-elastic material and an ideal solid. (Adapted from Schramm, 1994)

The ratio of the applied shear stress to the maximum strain is called the “complex modulus” (G^*) and is a measure of a material’s resistance to deformation

$$G^* = \frac{\tau_0}{\gamma_0} \quad (3.13)$$

The complex modulus can be divided into an elastic and viscous portion representing the magnitude of the strain in-phase and out-of-phase with the applied stress, respectively. The elastic component is called the “storage modulus” and defined as,

$$G' = \left(\frac{\tau_0}{\gamma_0} \right) \cos(\delta) = G^* \cos(\delta) \quad (3.14)$$

The viscous component, or “loss modulus” is defined as’

$$G'' = \left(\frac{\tau_0}{\gamma_0} \right) \sin(\delta) = G^* \sin(\delta) \quad (3.15)$$

The complex modulus and phase angle can be expressed as functions of the storage and loss moduli:

$$G^* = G' + iG'' \quad (3.16)$$

$$\tan(\delta) = \frac{G''}{G'} \quad (3.17)$$

The “complex viscosity” (η^*) can be defined as,

$$\eta^* = \frac{G^*}{\omega} = \frac{G' + iG''}{\omega} = \eta' + i\eta'' \quad (3.18)$$

Where η' is the “dynamic viscosity” associated with the viscous response and η'' is the “storage viscosity” associated with elastic response. In the linear visco-elasticity region, the rheological parameters (G' , G'' , η^* , phase angle, δ) are expected to be independent of the magnitude of the applied stress.

3.5.2 Creep-recovery Test

In comparison to the oscillatory test, which focuses on the effect of shear stress on the visco-elasticity, the creep and recovery test introduces an additional parameter of the ‘effect of time’ to the viscous and the visco-elastic behaviour of suspensions.

In a creep recovery test, the shear stress is applied instantaneously to the sample and the strain is then monitored as a function of time as illustrated in Figure 3.9. After a pre-set time (usually seconds, the choice of time period depends on the material) the stress is removed and the strain induced in the sample is recorded.

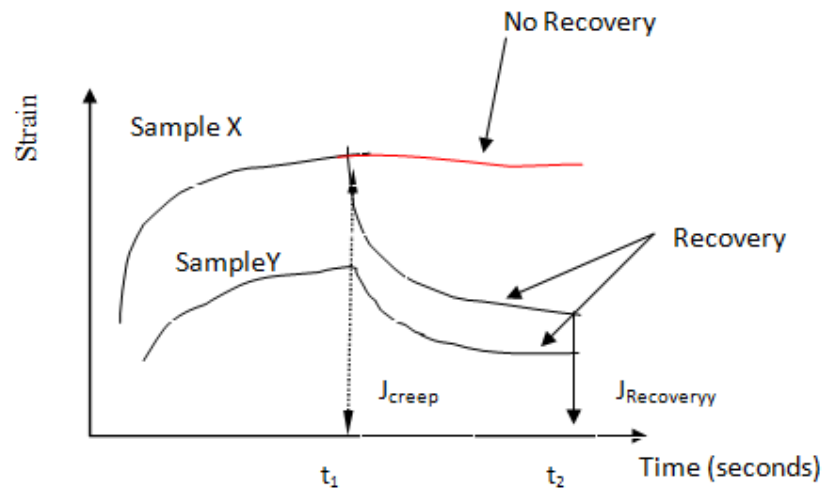


Figure 3.9: Schematic of creep-recovery response profile from a visco-elastic material

The resulting creep curve obtained after the stress has been removed can be divided into two regions, as shown in Figure 3.9. The first region

represents the measured deformation for a period t_1 , for a constant applied stress, whilst the second region represents the recovery of the sample after the applied stress has been removed. Assuming the applied stress is constant, sample X experiences a much higher deformation compared to sample Y. Once the pre-set time of t_1 is reached, the applied stress is removed and the recovered strain is monitored until t_2 . For the creep-recovery test, one of the key requirements is that the applied shear stress should be within the linear visco-elastic region (LVR). In the creep-recovery test, the compliance (J_{creep} and J_{Recovery}) of the material are measured; note that the compliance is the ratio of the strain, γ in the sample to the applied stress τ as given by equation below:

$$J = \frac{\gamma}{\tau} \quad (3.19)$$

If the sample does not recover to its original structure (complete recovery) after the removal of stress, the curve in Figure 3.9 labelled as ‘no recovery’. An elastic material will tend to recover some of the deformation depending on the extent of deformations. The test can be used for studying low shear phenomenon in paste materials; such as slumping (Costello, 1997).

3.6 Correlation of viscosity with volume fraction

In the rheological studies, several empirical models can be found that describe the relationship between the relative viscosity (η_r) of the suspension

and the solids powder content expressed by volume fraction. The relative viscosity (η_r) is defined as the quotient of the apparent viscosity of the suspension ($\eta_{\text{material paste}}$) and the pure binder (η_{resin}). Einstein showed in 1906 that with increasing solids powder content the viscosity of the suspensions increases (Einstein, 1906):

$$\eta_r = 1 + 2.5\phi \quad (3.20)$$

The Einstein relationship is valid for diluted solutions and requires the solid particles to be spherical with an identical radius (Einstein, 1906 and Batchelor, 1970). With the integration and expansion of Einstein's equation, a large number of empirical models have been developed for a correlation of the relative viscosity with solids content, namely Krieger-Dougherty model, Quemada model and Eilers model (Eilers, 1941; Krieger and Dougherty, 1959; Quemada, 1977):

Krieger-Dougherty model:

$$\eta_r = \left(1 - \frac{\phi}{\phi_m}\right)^{-[\eta]\phi_m} \quad (3.21)$$

Quemada model:

$$\eta_r = \left(1 - \frac{\phi}{\phi_m}\right)^{-2} \quad (3.22)$$

Eilers model:

$$\eta_r = 1 + \left(\frac{1.25\phi\phi_m}{\phi_m - \phi}\right)^2 \quad (3.23)$$

With η_r relative viscosity, ϕ volume fraction, ϕ_m maximum packing factor, and $[\eta]$ intrinsic viscosity of the suspension ($[\eta]=2.5$ for spheres). And noted

$$\text{that } \eta_r = \frac{\eta_{suspension}}{\eta_{medium}}. \quad (3.24)$$

The viscosity of the suspensions, considering particles as rigid spheres, is directly related to the volume fraction. In suspensions with high-powder (fillers) concentration, the interactions between the particles affect the overall rheological behaviour. This is because, at high concentration ϕ , viscosities become sensitive to small variations in particle properties such as surface roughness, size distribution, shape and arrangement of the particles. In particular, when particles of two differing sizes are mixed, the viscosity can be much more lower than it is for suspensions containing the same volume fraction of monosized particles. Maximum packing factor ϕ_m is the highest volume of particles that can be added to a fluid until the flow of suspension is blocked (Barnes et al, 1989 and Mewis et al., 2009).

Chapter 4

MATERIALS AND METHODS

4.1 Introduction

This chapter presents a description of the sample formulation, experimental equipment and the parameters used for different parts of the study.

4.2 Isotropic Conductive Adhesives (ICAs)

The ICAs consist of 70-80% metal fillers dispersed in an epoxy resin. During curing, the epoxy resin shrinks, which enables the metal fillers to come into contact hence conducting electricity. There are various types of metal fillers e.g. silver, nickel, gold, copper, carbon and metal-coated particles. The most commonly used metal filler is silver flakes or particles. Silver is preferred to other metal fillers because of its unique characteristic to conduct electricity even after it oxidises. When the adhesive is cured the filler particles are uniformly distributed and form a network within the polymer structure. From these networks, electricity can pass through making the mixture electrically conductive and due to nature of the network, the current can flow in any direction. The ICAs generally consist of resin such as epoxy (most commonly), polyamides, silicones and acrylic adhesives.

4.3 Materials and sample preparation

ICA generally consists of two elements:

- 1) Epoxy resin (DGEBA)
- 2) Metal fillers (silver flakes and silver nano-powders)

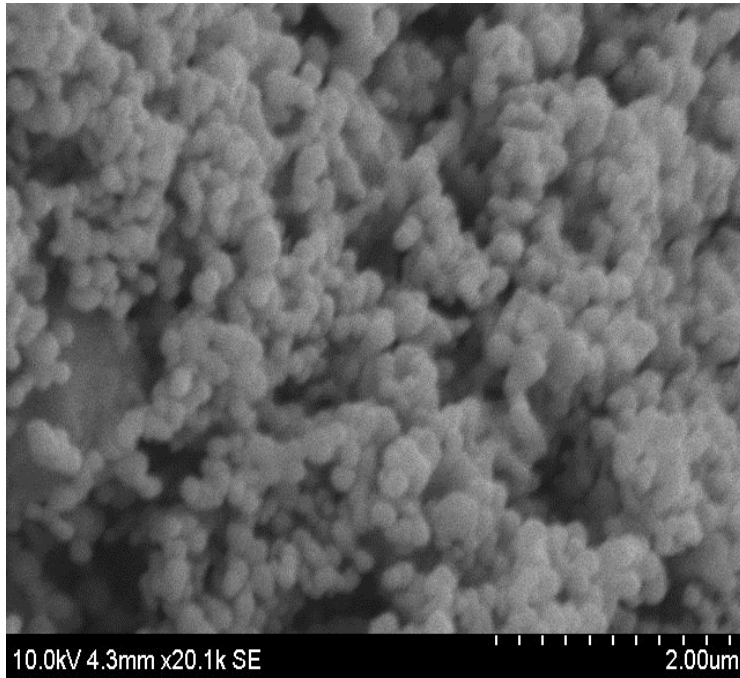
The variable of the ICAs paste are the filler contain and the weight fraction of the ICAs paste are shown in Table 4.1 and 4.2. In this study, three set of sample will be formulated which are silver powder will be added as filler contain of the ICAs paste, ICAs paste with only consists of silver flakes as filler contain and mixture of silver flakes and silver nano-powders. The silver flakes and silver nano-powder were not treated in this work. The SEM images of the silver flakes and silver nano-powder are shown in Figure 4.1. An X-ray diffraction test was conducted on the silver flakes and powder; the phases in Figure 4.2 show the existence of Ag only. Thus, it confirmed that the material is pure silver.

Table 4.1: ICAs Formulation with silver flakes

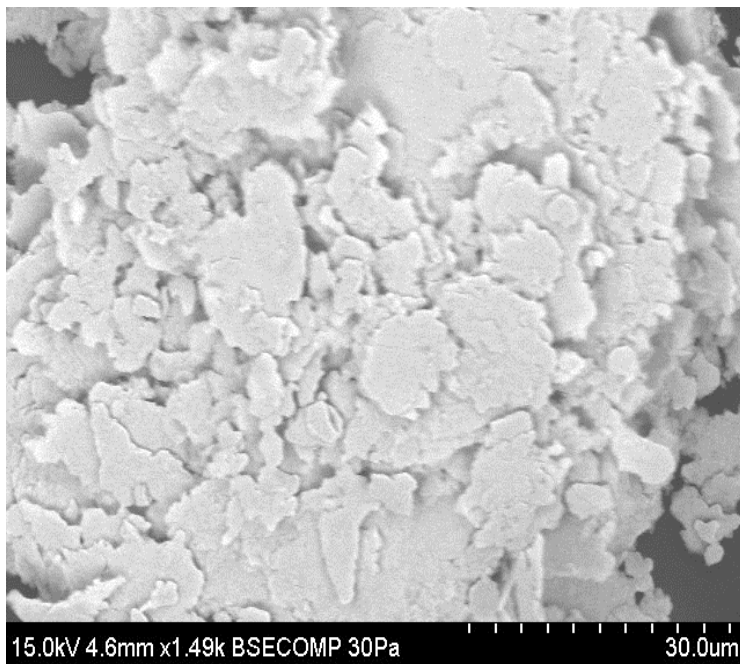
Paste	Weight Fraction	Weight (grams)	Material
A	0.8wt%	8	Silver Flakes
		2	DGEBA
B	0.6wt%	6	Silver Flakes
		4	DGEBA
C	0.4wt%	4	Silver Flakes
		6	DGEBA
D	0.2wt%	2	Silver Flakes
		8	DGEBA

Table 4.2: ICAs Formulation with silver flakes and silvernano-powder

Paste	Weight Fraction	Weight (grams)	Material
E	0.8wt%	0.4	Silver Nano-powder
		7.6	Silver Flakes
		2	DGEBA
F	0.6wt%	0.3	Silver Nano-powder
		5.7	Silver Flakes
		4	DGEBA
G	0.4wt%	0.2	Silver Nano-powder
		3.8	Silver Flakes
		6	DGEBA
H	0.2wt%	0.1	Silver Nano-powder
		1.9	Silver Flakes
		8	DGEBA



(a)



(b)

Figure 4.1 SEM Microstructure of (a) Silver nano-powders and (b) Silver flakes

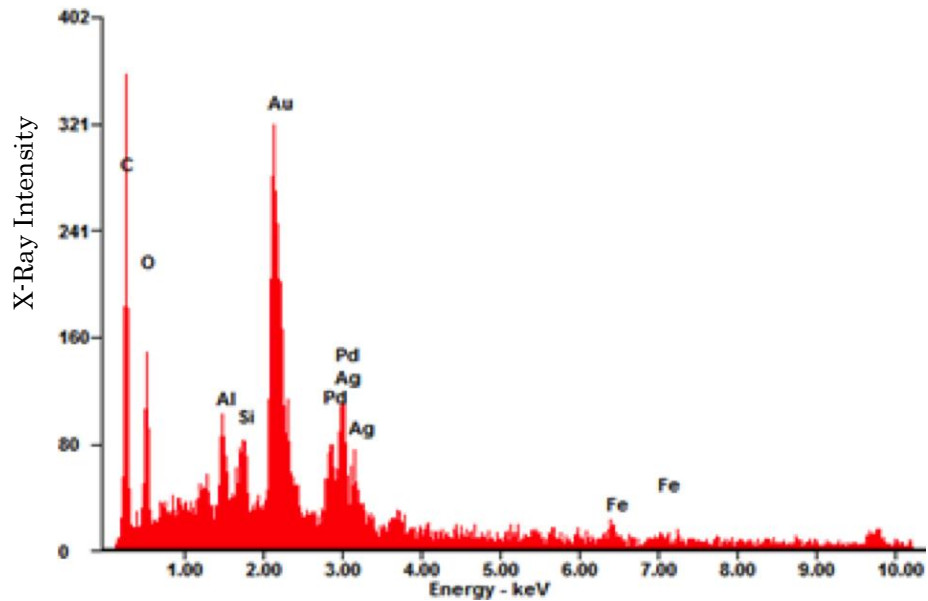


Figure 4.2 EDAX pattern for silver (Ag)

4.4. Rheometry

Rheometry refers to a set of standard techniques that are used to experimentally determine rheological properties of materials (fluid or solid). A rheometer can be used to exert a torque/force on a material; and to accurately measure its strain with time (or conversely, it can be used to impose a strain and measures the resulting torque). In rotational rheometry, the following assumptions are made (Walter and Kemp, 1969):

- 1) the equations of motion are valid,
- 2) the boundary conditions are known,
- 3) a rheological model is applicable,
- 4) a velocity gradient occurs within the sample.

Assumption (3) is used to provide the theoretical basis for the understanding of the viscometric flows. Assumption (4) is used for the analysis of experimental data and is the basis for many of the rheological apparatuses available today. For example, the rheological properties of a Newtonian fluid can be fully characterised by one parameter that is the viscosity. However, with non – Newtonian fluids the situation becomes more complex and it is no longer possible to fully characterise the fluid by viscosity alone – other fluid properties such as thixotropy and visco-elasticity are needed to describe fluid behaviour. The development of paste products such as solders pastes and conductive adhesives used in electronic packaging and interconnection requires a good understanding of the effect of rheological properties on the paste's processing performance.

4.4.1 Viscometry

Viscometry is a branch of rheometry, which is concerned, with the determination of the relationship between the shear stress and the shear rate of a fluid. Viscometric flow may be divided into two categories: 1) Poiseuille flows, and 2) Couette flows (Couette flows are also known as drag flows). In the first case the walls of the systems are stationary and the flow is caused by the application of external pressure to the fluid. In the Couette flow, there is no pressure difference, but one of the walls of the system moves in such a way as to cause fluid flow. In fact the fluid is dragged along with the wall because of the action of viscous forces

There are a number of factors, which makes it impossible to develop a full viscometric flow in practice, and these depend greatly on the nature of the fluid under examination. For example, suspensions such as solder paste could be affected by factors such as boundary effects and end effects, which may strongly influence the results.

The two most popular tools that are used to generate Couette flow are the cone and plate and parallel plate geometries. As illustrated in Figure 4.3, the viscometric flows in the parallel plate and rotating the top plate generates the cone and plate, while the bottom plate remains stationary.

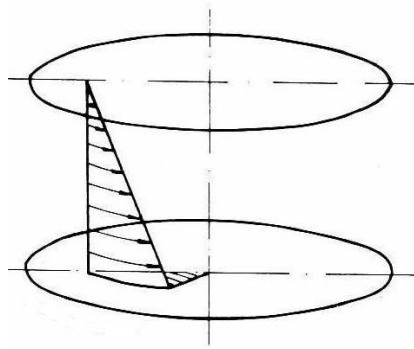


Figure 4.3 Couette flow in the parallel plate geometries

4.4.2 Geometries Utilised for Rotational Rheometry

In a rheometer, the test sample under study is placed in between the instrument geometries (the parallel plates). One plate is driven at a pre-defined angular velocity, ω , while the other plate is kept stationary. Two different techniques can be used to generate shear, controlled shear rate and controlled shear stress. In controlled shear rate instruments, one of the shearing surfaces is driven at a pre-selected speed while the other is restrained by a torsion bar or spring with known deflection characteristics. In contrast, the controlled

stress rheometer applies a controlled torque, and hence shears stress, to the test sample.

4.4.3 Parallel Plate Geometry

In the parallel plate geometry, Figure 4.4, the sample is sandwiched between two plates separated by distance, h ; one of the plates rotates at constant angular velocity, ω , while the other plate is held stationary. Assuming that steady simple shear flow is attained between the two plates and that inertia and end effects are negligible, then the shear rate ($\dot{\gamma}$) induced in a parallel plate will be proportional to the radius (r) of the plate, and is given by:

$$\dot{\gamma}_r = \frac{\omega r}{h} \quad (4.1)$$

where r is the radius of the plate, ω is the angular velocity, and h is the gap height between the two plates.

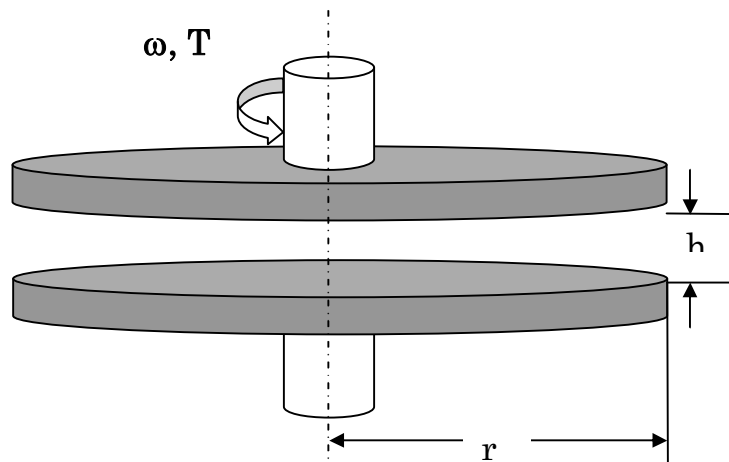


Figure 4.4 Parallel-plate geometry

Since the shear rate is not constant across the radius of the plate, an equation to relate shear stress to torque measurements is needed. The shear stress is given as:

$$\sigma = \frac{2T}{2\pi r^3} \left[3 + \frac{d \ln T}{d \ln \dot{\gamma}_r} \right] \quad (4.2)$$

Where σ = shear stress, T = total torque

In a study reported by Walter and Kemp (1969), which concern the comparison of different plate geometries, they suggested that the advantage of using the parallel plate geometry was because the gap height can be varied to accommodate the fluid. In contrast to cone and plate geometry, the parallel plate overcomes particles jamming, making it the most favoured geometry for solder paste rheological measurements.

For both cone and plate and parallel plate geometries certain assumptions are made to determine the total force acting on the plate. These assumptions include the following:

- 1) Inertial effects are negligible, i.e. the fluid density is zero.
- 2) The cone angle is very small so that a uniform velocity profile is generated across the radius of the plate.
- 3) The free surface of the liquid is part of a sphere (cone) or cylinder (parallel) of radius r (r = radius of plate).
- 4) Surface tension is negligible.
- 5) The flow is laminar and thus continues up to the fluid surfaces, i.e.

edge effects can be neglected.

4.5 Rheometer

In this study, rheometer plays an important role in obtaining data through analyzing the material provided. The rheometer that will be used is Physica MCR301, as shown in Figure 4.5, with the parallel plate of 25 mm and gap of 1 mm as shown in Figure 4.6. A vibration free platform is needed for rheometer, since rheometer is very sensitive instrument; it's to avoid the inaccuracy and disturbance of the result obtain. The sample pastes will be placed at the bottom plate while the top plate will then be lowered to the desired height 1 mm. As the top plate lowered to 1 mm height, the excess sample will be squeezed out and will need to be trimmed by using a plastic spatula. The sample then will be allowed to rest for about 1 minute before the test commences. This loading procedure is identical to all other test and all tests will be conducted at the room temperature. All tests were conducted at 25°C with the temperature being controlled by a Peltier-Plate system. At least two replicates of each test were performed.



Figure 4.5 Physica MCR301 rheometer

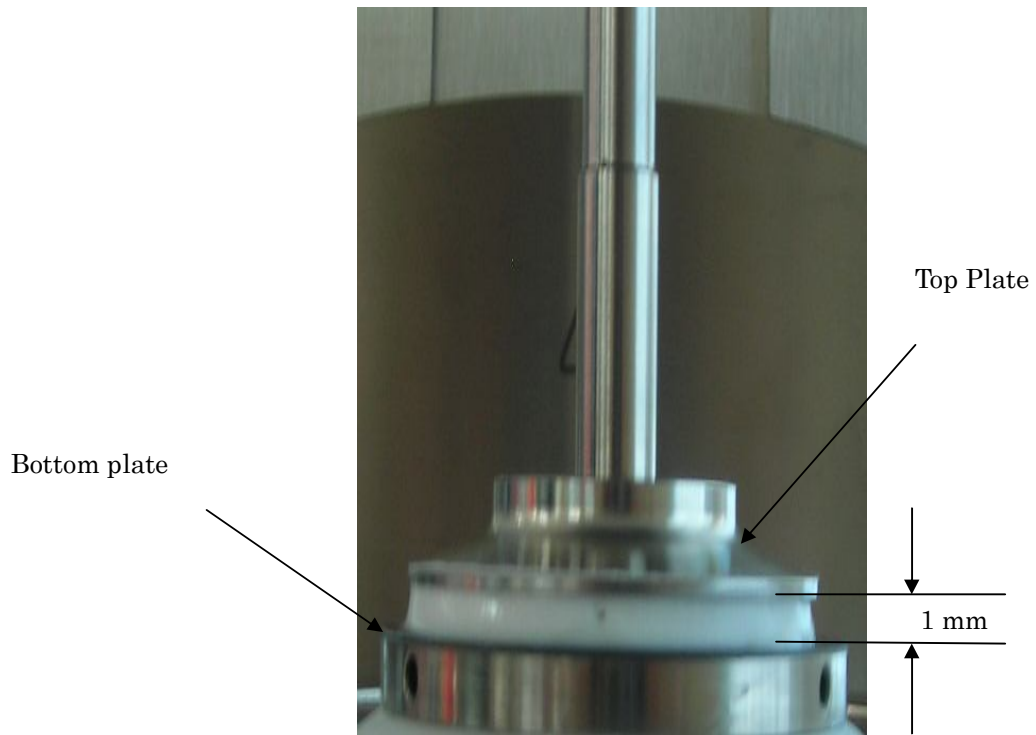


Figure 4.6 Parallel Plate of Physica MCR301 rheometer

Chapter 5

THIXOTROPIC STUDIES

5.1 Results and Discussion

5.1.1 Constant shear rate test

In this test, a constant shear rate of 0.01, 0.1, 1, 10, and 50 s^{-1} was applied to the ICA paste for 120 seconds. It should be noted that an equilibrium time of 300 seconds was used prior to the start of each test. Figure 5.1 shows the paste A (0.8 wt%: 0.8 wt% of silver flakes and 0.2 wt % epoxy), with reference to Table 4.1, under constant shear rate of 0.01, 0.1, 1, 10, and 50 s^{-1} . As for the constant shear rate of 0.01 s^{-1} , the viscosity reach the steady state of 276 000 Pa.s at 54 seconds over 120 seconds. For the constant shear rate of 0.1 s^{-1} , the viscosity increase slowly from 28 400 Pa.s to 34 900 Pa.s before it becomes steady state of which nearly a straight line in the diagram. The viscosity is not affected by the shear rate of 0.1 s^{-1} and 0.01 s^{-1} due to the agglomerations of the silver flakes within the mixture. This happens in a concentrated suspension due to close packed structure. For the constant shear rate from 1 s^{-1} , the viscosity of the paste reduces gradually until it reaches the end of 120 seconds. When the sample was subjected to 10 s^{-1} and 50 s^{-1} , the paste's viscosity to drop rapidly at the early stage and slows down as it approach steady state. Ideally, it is expected for the viscosity to remain constant for the period of 120 seconds. However, the material structure then to

breakdown over a period of time. The rapid drop in viscosity may be due to structural breakdown experienced by the paste.

When the paste B (0.6 wt%: 0.6 wt% of silver flakes and 0.4 wt% epoxy) were subjected to the same test parameters. A similar result was observed as paste A, as shown in Figure 5.2. This shows that the flow behaviour observed for both paste A and B is attributed to the silver flakes filler material. When weight fraction of the silver material was dropped to 0.4 wt % and 0.2 wt %, for paste C and D, as shown in Figure 5.3 and 5.4, the viscosity does not change for 1 s^{-1} , 10 s^{-1} and 50 s^{-1} . The drop in the filler weight percentage shows that the samples tend to behave more Newtonian than non-Newtonian. The higher shear rate does not influence the flow behaviour due to the low weight percentage of silver flakes. In low weight percentage systems such as paste C and D, the interaction of the silver flakes is low.

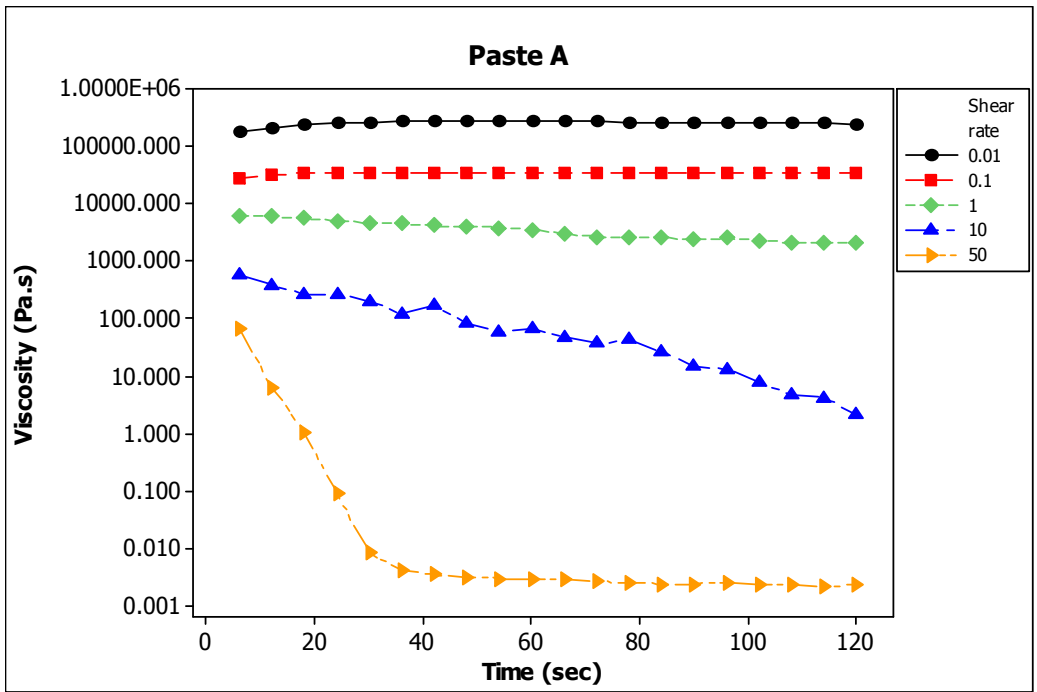


Figure 5.1: Effect of Constant Shear on Paste A

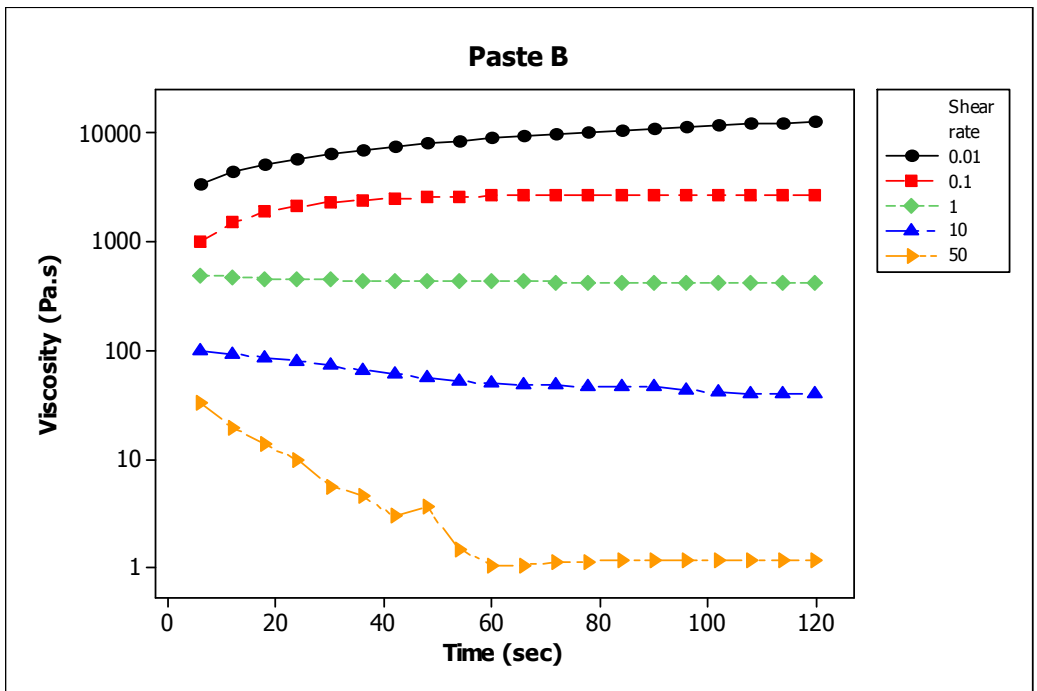


Figure 5.2: Effect of Constant Shear on Paste B

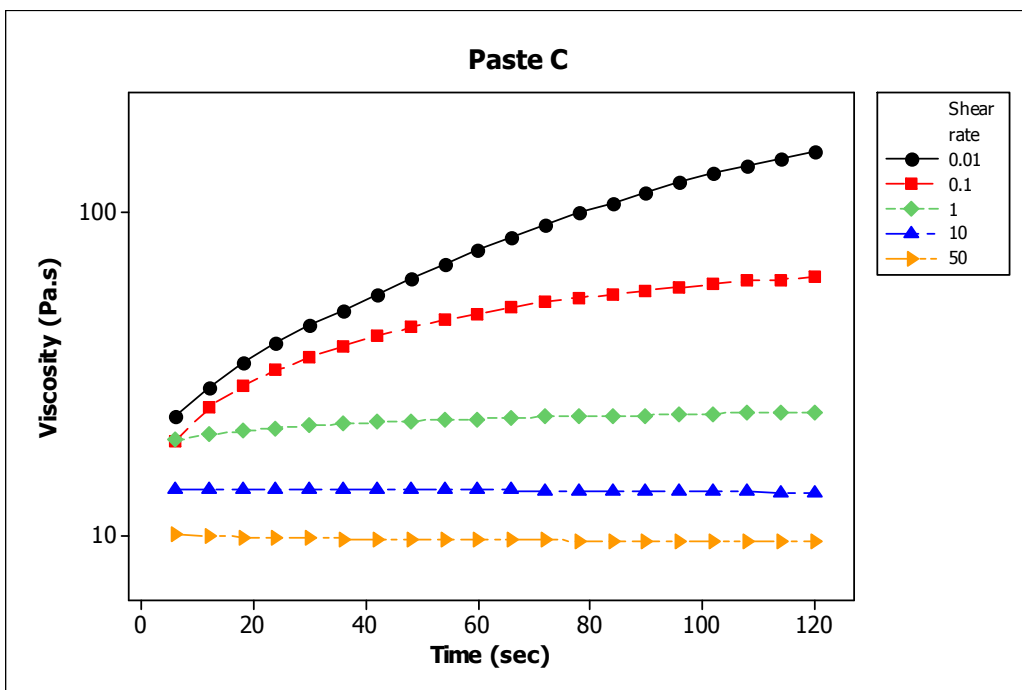


Figure 5.3: Effect of Constant Shear on Paste C

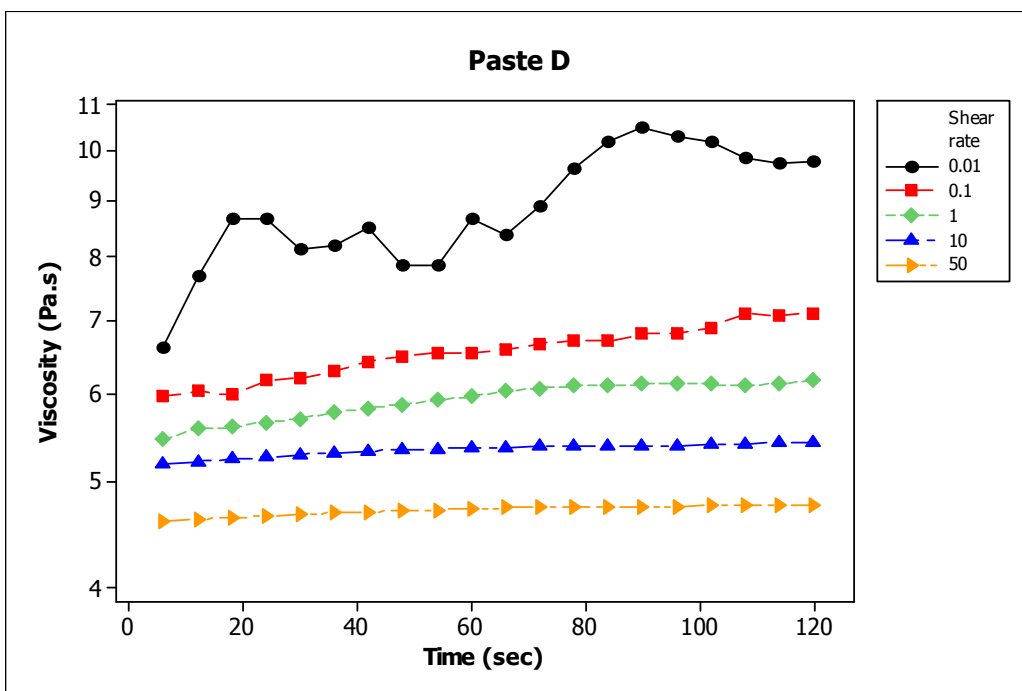


Figure 5.4: Effect of Constant Shear on Paste D

5.1.2 Viscosity of Mixture of Silver Flakes with Silver Nano-powder

A small percentage of silver flakes are replaced with silver nano-powder but the overall weight percentage, as listed in Table 4.2 is maintained for comparison with paste A, B, C and D, as listed in Table 4.1. The purpose of this experiment is to investigate how the result will be different when silver nano-powder is added to the mixture of paste E, F, G and H. The result will be shown in comparison with the result without silver nano-powder. For consistency, the same weight percentage will be compared.

In Figure 5.5, the viscosity of paste E and paste A is compared over constant shear rate of 0.01, 0.1, 1, 10, and 50 s^{-1} . Paste E tends to dominate over paste A in terms of viscosity over constant shear rate. When under constant shear rate of 10 s^{-1} , paste E gives better viscosity of 177 Pa. Meanwhile, both paste E and paste A experiencing structural breakdown when subject to constant shear rate of 50 s^{-1} . However, Figure 5.5 illustrated paste E has a slower breakdown than paste A. This may due to the mixture of paste E contains silver nano-powder which forms stronger intermolecular bonding before the shear rate could break the suspension into smaller flocculation over time (S Mallik et al, 2010).

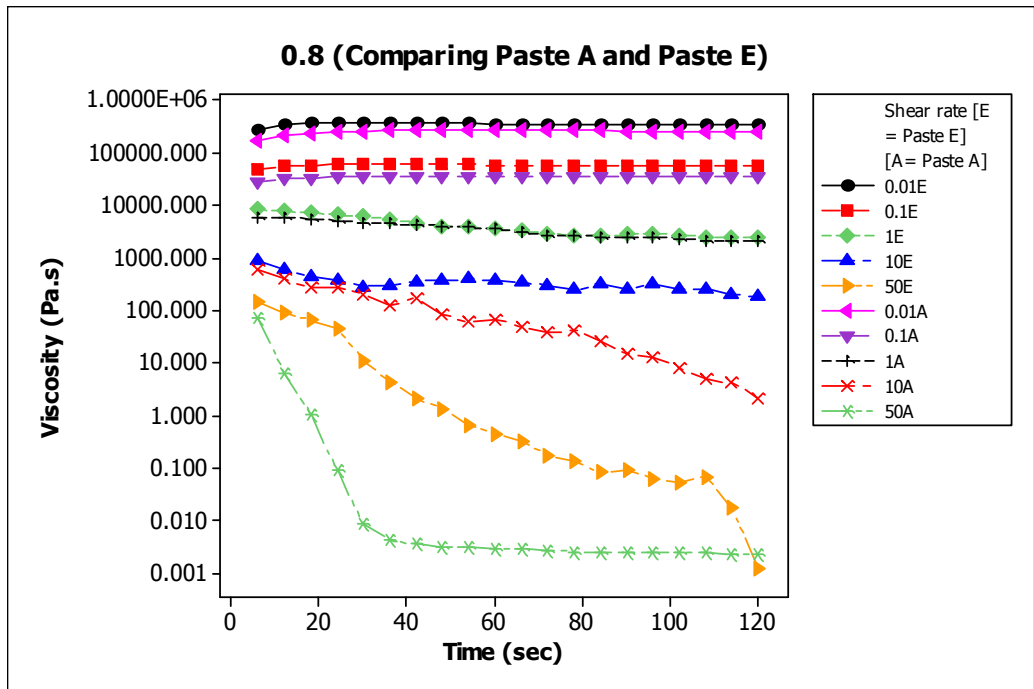


Figure 5.5: Constant shear rate for Paste A and Paste E

Figure 5.6 shows the comparison of viscosity for paste B and paste F over constant shear rate of 0.01, 0.1, 1, 10, and 50 s⁻¹. For 0.01 until 1 s⁻¹, the result obtained very similar trend, but when paste F under constant shear rate of 10 s⁻¹, the viscosity of paste F drop below the paste B at the 102 seconds where paste F is 39.6 Pa.s and paste B is 40.5 Pa.s. As observed for paste A and E, the presence of nano-powder increases the viscosity of the suspension but for the case of paste B and F this was not the case. When both paste B and paste F under constant shear rate of 50 s⁻¹, Paste F experiencing incredible structural breakdown which exceeding paste B over 1.1468 Pa.s. This could be due to lower weight percentage of 0.6, hence the amount filler is lower compared to weight fraction of 0.8.

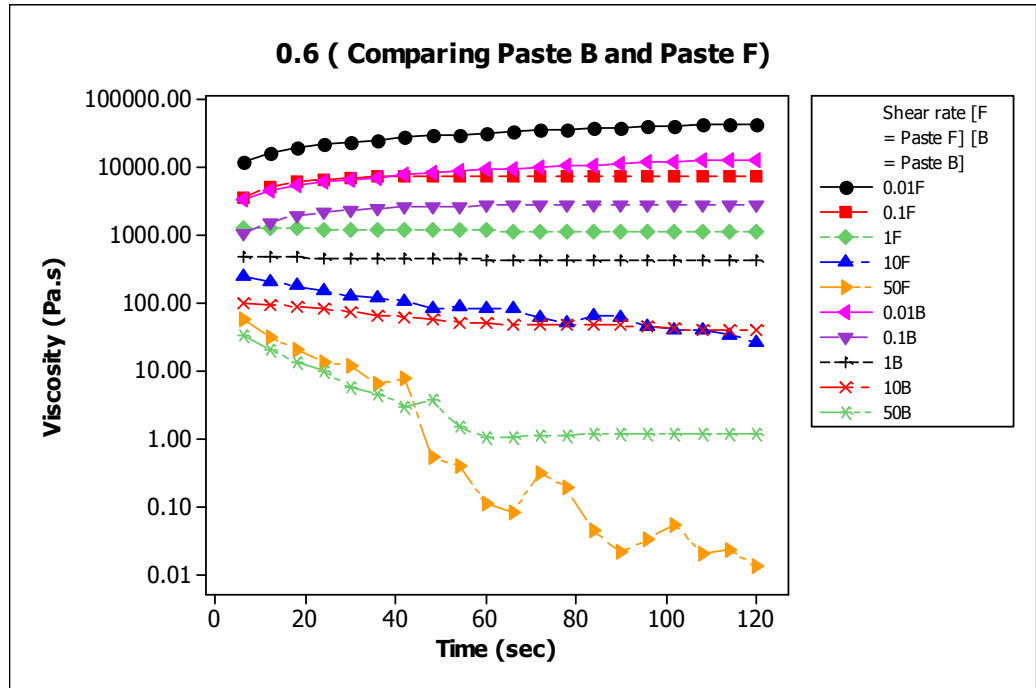


Figure 5.6: Constant shear rate for Paste B and Paste F

Figure 5.7 shows that paste G only have higher viscosity than paste C when paste G under constant shear rate of 0.01 s^{-1} . When paste G undergoing higher shear rate, the viscosity obtain is lower than the paste C that is without silver nano-powder. Just like the result of paste C and D, which have higher weight fraction of epoxy then conductive filler, the paste does not experiences structural breakdown. Figure 5.8 show that the silver nano-powder that added into the mixture does not affect the viscosity when under constant shear rate $0.01, 0.1, 1, 10, \text{ and } 50 \text{ s}^{-1}$. When paste H (with silver nano-powder) under

constant shear rate as mention above, the viscosity of the paste H is lower than the paste D (without silver nano-powder). Figure 5.7 and 5.8 concluded that when the polymer resin of the paste have higher weight fraction over conductive filler, the silver nano-powder that added into the mixture does not increase the viscosity of the paste when under same constant shear rate as the mixture that only contain silver flakes.

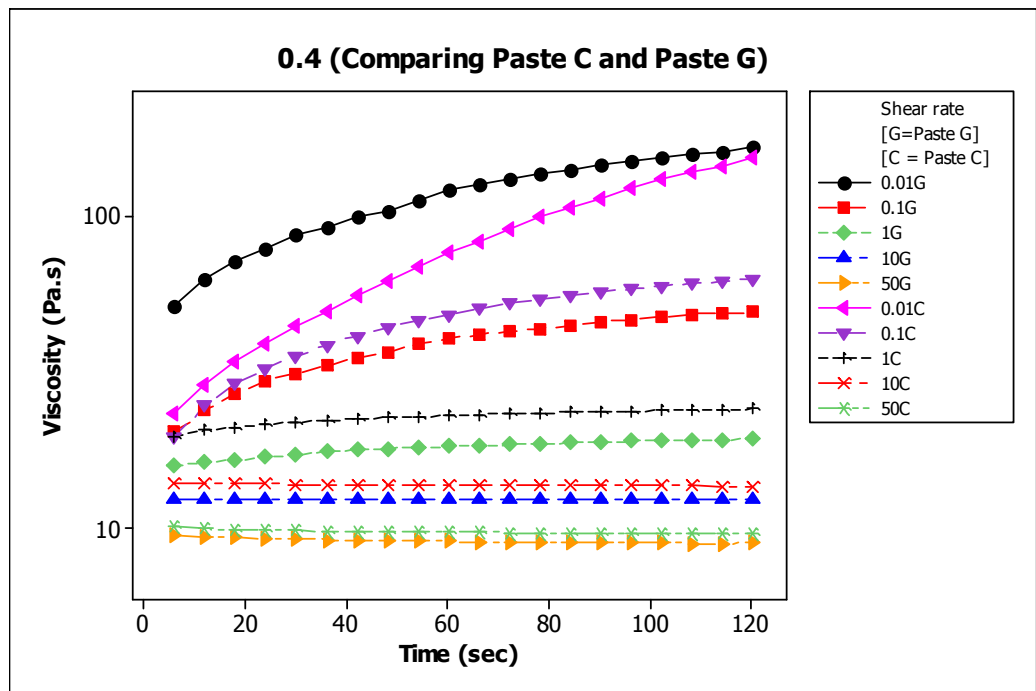


Figure 5.7: Constant shear rate for Paste C and Paste G

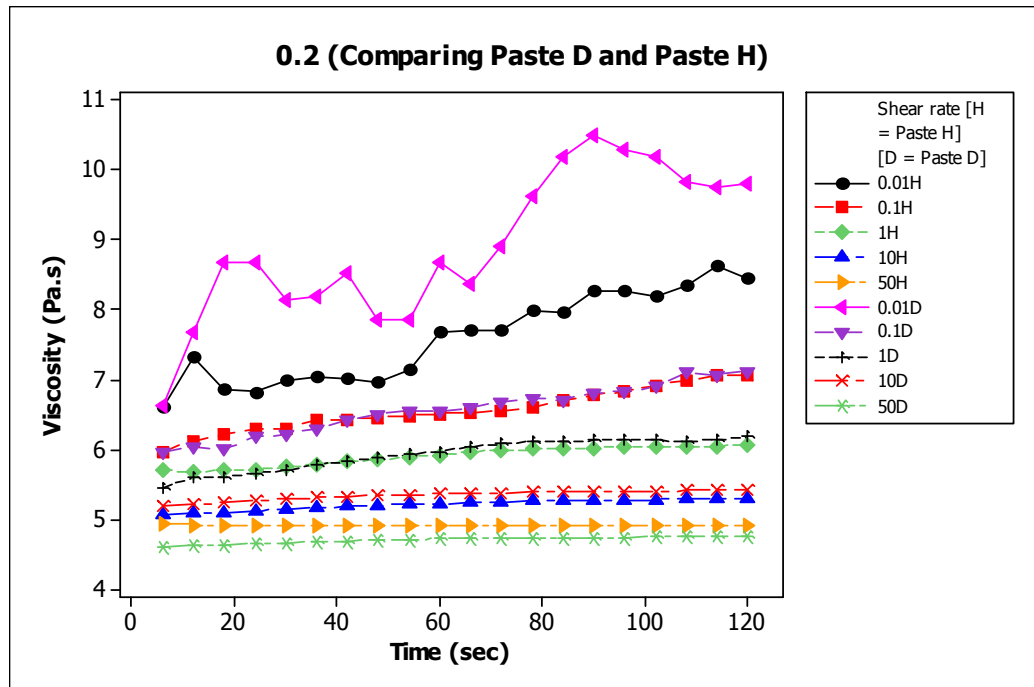


Figure 5.8: Constant shear rate for Paste D and Paste H

5.1.3 Results from Hysteresis Loop Test

By using the pastes of A to H (please refer to Tables 4.1 and 4.2), the thixotropic behaviour of the formulated ICAs with silver flakes and silver nano-powder was investigated through conducting the hysteresis loop test. All the pastes display thixotropic behaviour as there are hysteresis loop present between the step-up curve (0.01 to $10s^{-1}$) and step-down curve (10 to $0.01s^{-1}$). The region between the step-up and step-down curves is the indication the existence of thixotropic behaviour in that particular paste. The recovery percentage of the paste between the step-up (break down) and step-down (build-up) can be calculated by using the formula of:

$$\text{Recovery (\%)} = 100\% - \left\{ \frac{[\text{Viscosity (rest)} - \text{Viscosity}(\text{recovery})]}{\text{Viscosity (rest)}} \times 100\% \right\}$$

From the observation of Figure 5.9, Paste E has higher value of viscosity over paste A no matter during either step-up curve (structural breakdown) or step-down curve (structural build-up). The calculation for the recovery percentage for paste E is higher than paste A from every prospect of shear rate (from 0.01 to 10s^{-1}). Paste E has 20.6%, 6.3%, 8.1%, and 11.7% more recovery than paste A during shear rate of 0.01, 0.1, 1, and 10 s^{-1} . At 0.8 wt%, the presence of silver nano-powder within the pastes shows a higher degree of thixotropy.

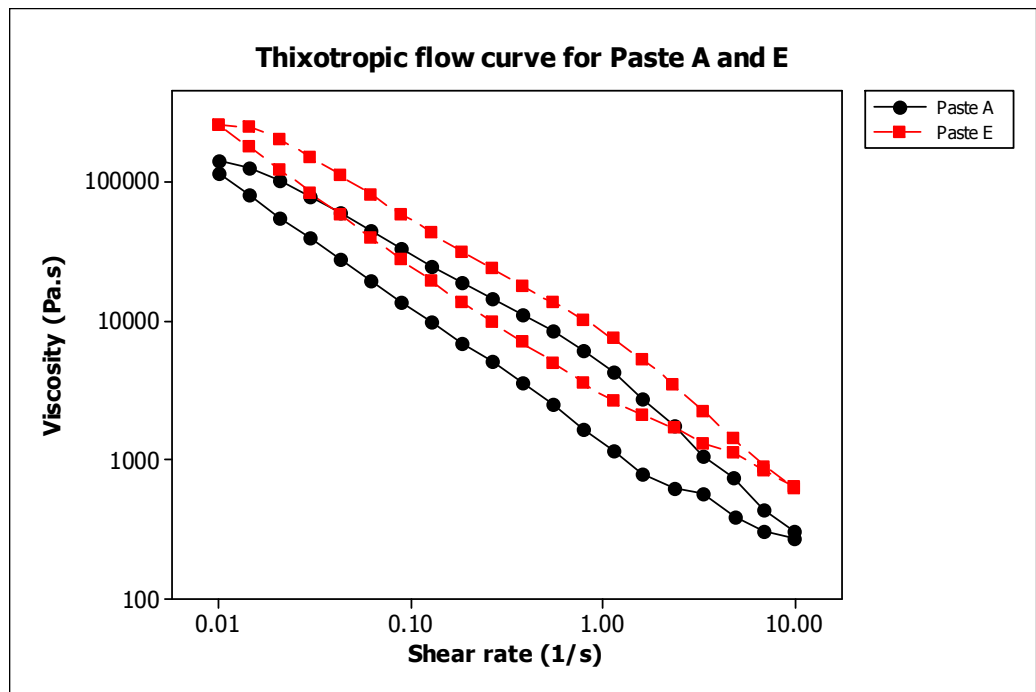


Figure 5.9: Hysteresis flow curve of Paste A and E

Figure 5.10, paste B shows an extreme recovery rate during the final

point of 0.01 s^{-1} . It indicates that pastes that share the same shear rate will yield higher viscosity if the shear stress is higher. It clearly shows that the shear stress during the shear rate of 0.01 s^{-1} for paste B during the build-up process is much higher than the shear stress during breakdown process at shear rate of 0.01 s^{-1} . This could indicate that higher viscosity is due to higher shear stress applied within the suspensions. Paste B dominates paste F in terms of recovery percentage of 30.99%, 27.93 %, and 14.09% at the shear rate of 0.1, 1, and 10 s^{-1} . Even though the recovery rates of the paste F do not as high as paste B, the overall viscosity for paste F is still higher than paste B.

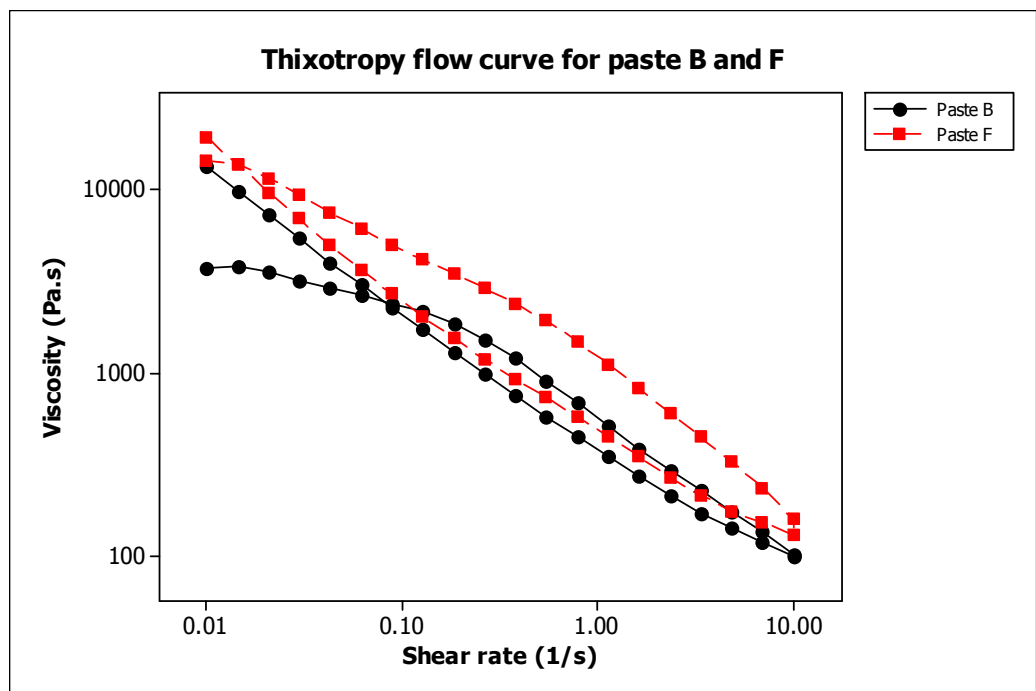


Figure 5.10: Hysteresisflow curve of Paste B and F

Figure 5.11 and Figure 5.12 indicate that paste C, D, G and H appears

to be nearly zero thixotropy behaviour due to very small hysteresis loop. The insignificance of hysteresis loop means that paste C, D, G, and H does not experience structural breakdown.

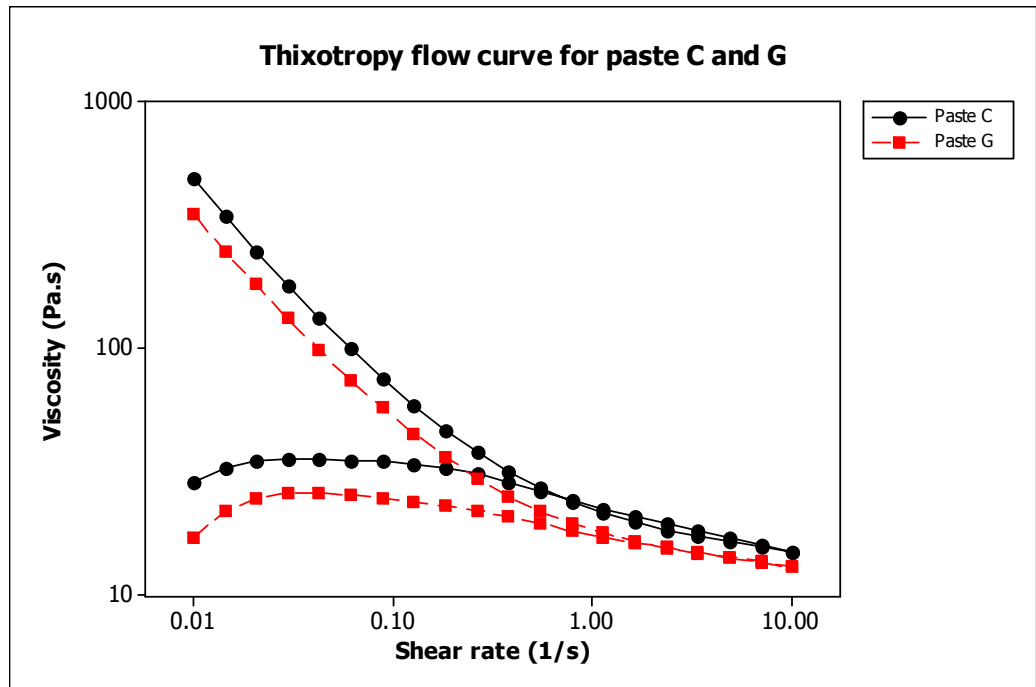


Figure 5.11: Hysteresis flow curve of Paste C and G

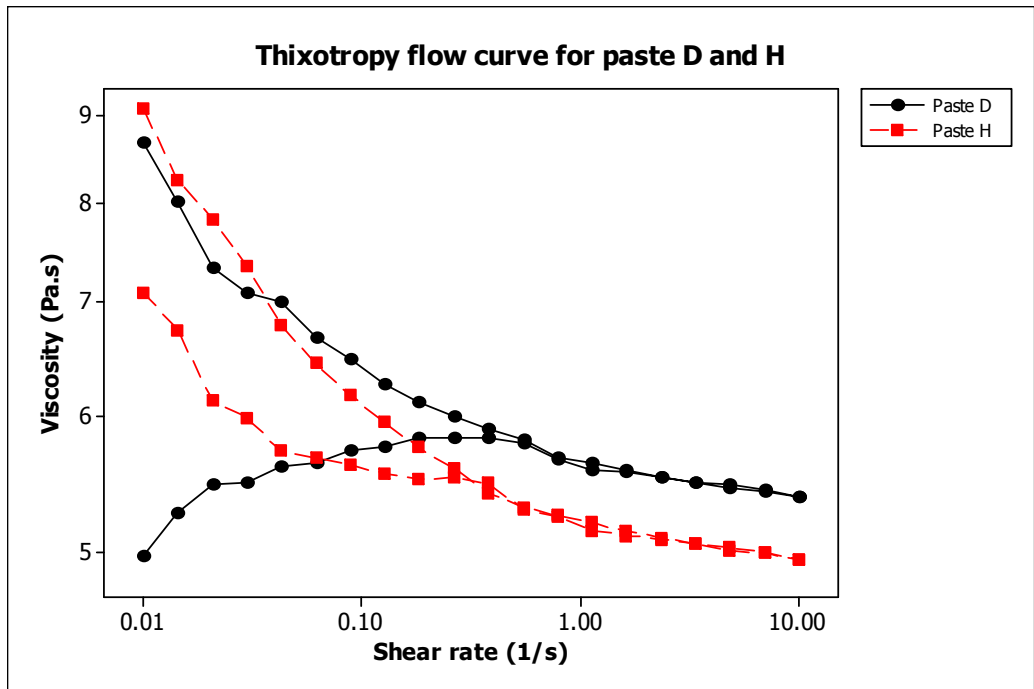


Figure 5.12: Hysteresis flow curve of Paste D and H

As shown in Figure 5.13, the recovery percentage for paste C, D, G and H above 80% between the shear rate of 1 to 10 s^{-1} (where there is a very small hysteresis loop between the shear rates). By comparing the same weight fraction of the pastes, which are 0.6wt% sample B and sample F, results shown that sample F give a better recovery rate compare to sample B. For sample A and sample E shown the, sample E gives a better recovery rate compare which sample A. These results indicate that the sample pastes which have the smaller particle (sample E and sample F) shown a better recovery condition. The results show that smaller filler size leads to large surface area and better inter-particle attraction. As the weight fraction of filler increases, the viscosity of the sample pastes increase as well. The initial viscosity is lower than the final viscosity which may due to the cohesive behaviour of the paste that increase

the resistance to the flow of the paste and after the paste experiencing the breakdown, the paste build-up more quickly due to the aggregation and Brownian movement of the particles within the suspension(Man, 2009).

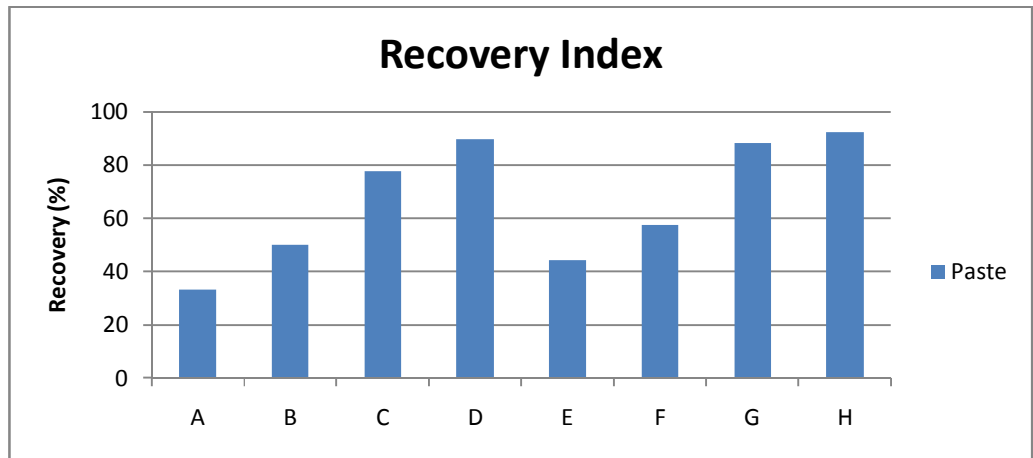


Figure 5.13 Recovery Index for Paste A to Paste H

Chapter 6

CREEP-RECOVERY AND OSCILLATORY SHEAR FLOW STUDIES

6.1 Results and Discussion

6.1.1 Creep Recovery test

In order to get the result of creep recovery, stress is applied on formulated samples for a period of time and later release in order for it to recovery itself. In other words, creep recovery involves a tensile specimen under constant load maintained at a constant temperature. The measurement of the strain will be recorded start from when the stress applied on the conductive adhesive until it recovery itself. The degree of sample movement is recorded against time as angular displacement, strain or compliance. In the graph we obtain, we use strain versus time. From the result we obtained from rheometer, compliance, J can be calculated using the formula. There are all together 3 compliances. From this, we can know the material's deformation index, creep recovery index and ratio of strain to stress applied.

From the graph we obtained from rheometer, the shape of the graph for each specimen is about the same. The graph curve increase to recovery point at 120 seconds when stress applied on it. When the stress is removed, the graph curve starts to decrease from 120 seconds to 240 seconds. For this test,

there are 2 types of test materials. The first material is silver flakes based conductive adhesive and the second material is silver flakes plus silver nanopowder based conductive adhesives. For silver flakes and silver flakes with nano-silver powder conductive adhesives, 10 Pa was applied for 0.2, 0.4, 0.6 and 0.8 wt%. For the initial strain, the 0.2 wt% had the highest strain value compared to the other specimens.

From Figure 6.1 and 6.2, specimen that has 0.2 wt% filler contain has the highest elastic behaviour compared to all the specimens. According to the result obtained, not all specimens were able to recover. Only silver flakes with 0.6wt% and 0.8 wt% filler contain and silver powder plus silver flakes with 0.8wt% filler contain had recovery. The compliance values, deformation and recovery index that we obtain from each specimen will be shown in Tables 6.1 and 6.2.

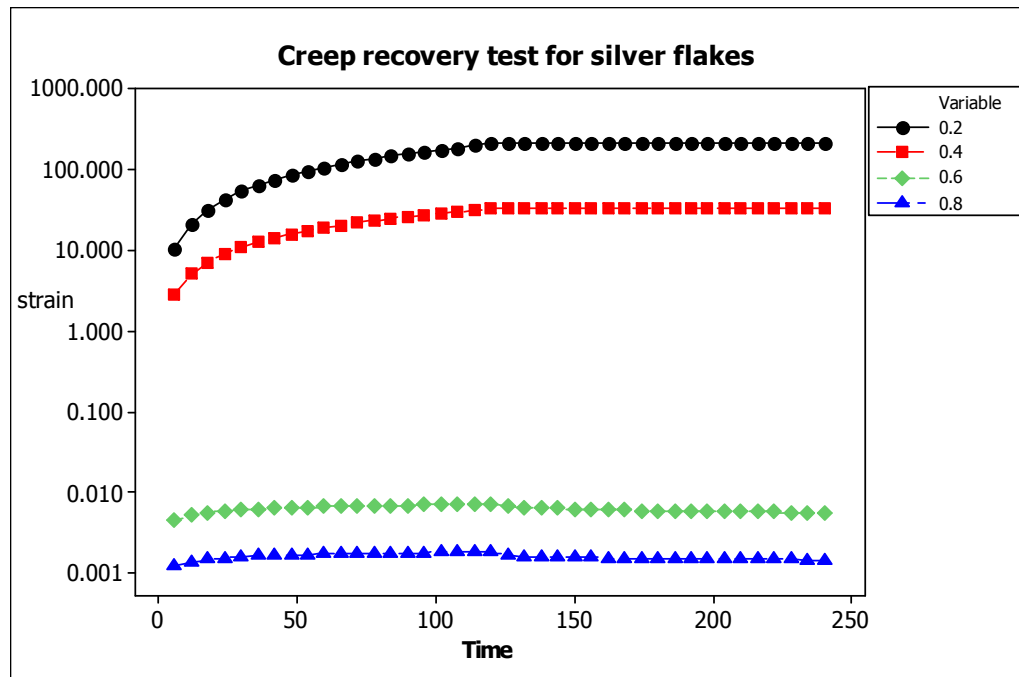


Figure 6.1 Creep-recovery for silver flakes at 10 Pa

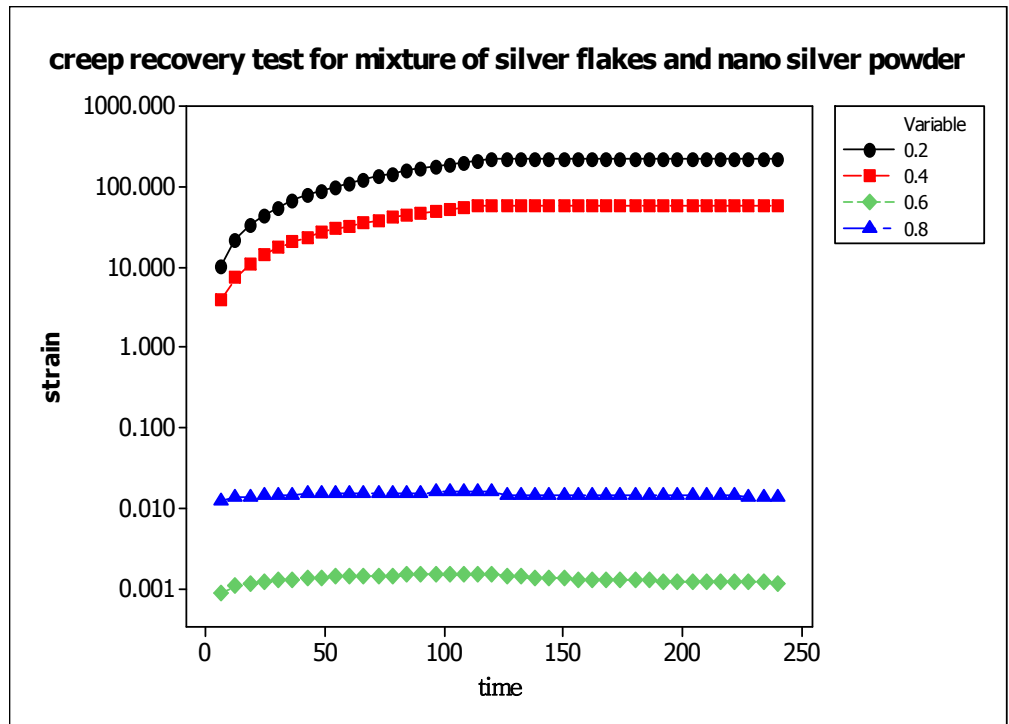


Figure 6.2 Creep recovery for mixture of silver flakes and silver nanopowder at 10 Pa

From the graph Figures 6.1 and 6.2 above, it had showed that the compliance value, J_1 , J_2 and J_3 for the 0.8wt% silver flakes and mixture of silver flakes and nano powder. By using this compliance value, deformation index, creep recovery index and ratio can be calculated using formula. Formula for measured compliance (J_1 , J_2 and J_3), as shown in Figure 6.3.

J_1 =Initiation point of strain/Applied stress

J_2 =Recovery point of strain/Applied stress

J_3 = Final point of strain/Applied stress

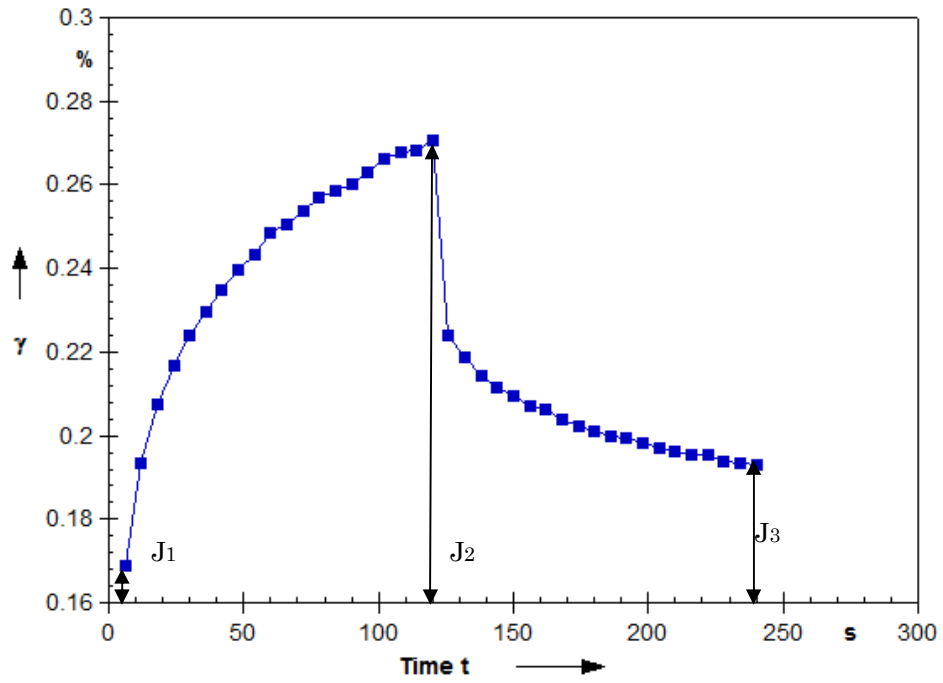


Figure 6.3 Compliance value of creep recovery graph

Table 6.1 Compliance data for silver flakes

Silver flakes	J1	J2	J3
A (0.8 wt%)	1.194×10^{-5}	1.824×10^{-5}	1.440×10^{-5}
B (0.6 wt%)	4.424×10^{-4}	7.123×10^{-4}	5.598×10^{-4}
C (0.4 wt%)	0.28	3.23	3.23
D (0.2 wt%)	0.98	20.11	20.17

Table 6.2 Deformation and recovery index for silver flakes ICAs paste from creep recovery result

Silver flakes	J2/J1 deformation index	J3/J2 creep recovery index	J3/J1 ratio
A (0.8 wt%)	1.528	0.789	1.206
B (0.6 wt%)	1.610	0.786	1.265
C (0.4 wt%)	11.543	0.999	11.529
D (0.2 wt%)	20.148	1.003	20.519

From the result that we obtained from the calculations, Tables 6.1 and 6.2, conductive adhesive with 0.2 wt% silver flakes showed the highest value of deformation index follow by 0.4 wt%, 0.6 wt% and 0.8 wt%. It showed that 0.2 wt% had the highest sample deformation at that applied stress. As for the creep recovery index, value that close to 1 implied that there is no recovery after the stress had been removed. Pastes C and D showed a creep recovery index value of 1.003 and 0.999 which close to 1. So, there are no recoveries. On the other hand, pastes A and B showed a creep recovery index values of 0.786 and 0.789, both of the specimens showed recoveries.

From the results we obtained from the calculations, Tables 6.3 and 6.4, although the filler contain of the conductive adhesive is different, but the result that we obtained also showed that 0.2 wt% specimen had the highest value of deformation index follow by 0.4 wt%, 0.6 wt% and 0.8 wt% specimens. But for the creep recovery index, only pastes E showed recovery. Pastes F, G and H showed recovery index value of equal to 1, so there are no recoveries for these 3 specimens.

Table 6.3 Compliance data for mixture of silver flakes and nano-silver powder

Silver flakes + nano silver powder	J1	J2	J3
E (0.8 wt%)	3.38×10^{-6}	5.42×10^{-6}	3.86×10^{-6}
F (0.6 wt%)	1.74×10^{-4}	3.06×10^{-4}	3.08×10^{-4}
G (0.4 wt%)	0.391	5.884	5.882
H (0.2 wt%)	1.044	22.19	22.34

Table 6.4 Deformation and recovery index for mixture of silver flakes and nano-silver powder

Silver flakes + nano silver powder	J2/J1 deformation index	J3/J2 creep recovery index	J3/J1 ratio
E (0.8 wt%)	1.604	0.712	1.142
F (0.6 wt%)	1.759	1.006	1.77
G (0.4 wt%)	15.018	0.999	15.013
H (0.2 wt%)	21.255	1.007	21.398

As from the results, pastes with 0.2wt%, 0.4wt% and 0.6wt% nano-silver powder fail to recover after the shear stress had been removed. But as for the silver flakes based isotropic conductive adhesive that, only 0.2wt% and 0.4wt% filler contain had no recoveries. But comparing the 0.8wt% silver flakes and 0.8wt% mixture of silver flakes and silver nano-powder, the result also indicated that the adding of silver nano-powder will give a better creep recovery rate. As indicated from the calculation table, the creep recovery index for ICA with silver flakes is 0.789 and ICA with mixture of silver flakes and silver nano-powder is 0.712. The presence of the silver nano-powder could improve the flow behaviour, which results in poor recovery. The nano particles could fill the voids between the silver flakes thus helping the sliding motion between the flakes.

6.1.2 Results from the Oscillatory Shear Test

The results from the oscillatory stress curves are shown in Figures 6.4-6.11. To analyse the oscillatory stress sweep plots, there are three areas that we will investigate. Firstly, to identify the linear region, secondly to determine the parameter of storage modulus, G' and loss modulus, G'' , and the last is the phase angle for all the ICAs. As we can see from the graph, ICAs with 0.8wt% silver flakes and 0.8wt% mixture of silver flakes and silver nano-powder had the linear visco-elastic region lies in 383-539Pa and 174-738Pa. As for ICAs with 0.6wt% silver flakes and 0.6wt% mixture of silver flakes and silver nano-powder showed a linear visco-elastic region lies in 1.59-7.47Pa and 6.44-29.4Pa. From this comparison, it indicated that adding silver nano-powder will enhance the linear visco-elastic region. The linear visco-elastic region can be defined as the maximum deformation that can be applied to the sample without destroying the structure. In this region, the particles stay in close contact with each other and recover elastically to any applied deformation. Beyond this region, the structure of the ICAs can be said that had been destroyed and therefore, the liquid characteristic will increase. As for the ICAs with 0.2wt% and 0.4wt% silver flakes and mixture of silver flakes and silver nano-powder showed that the loss modulus value, G'' is higher than the storage modulus value G' at the starting point to the end of the graph. This had indicated that both of these two ICAs materials are in liquid form. In this case, the Newtonian behaviour of the materials dominates the flow behaviour.

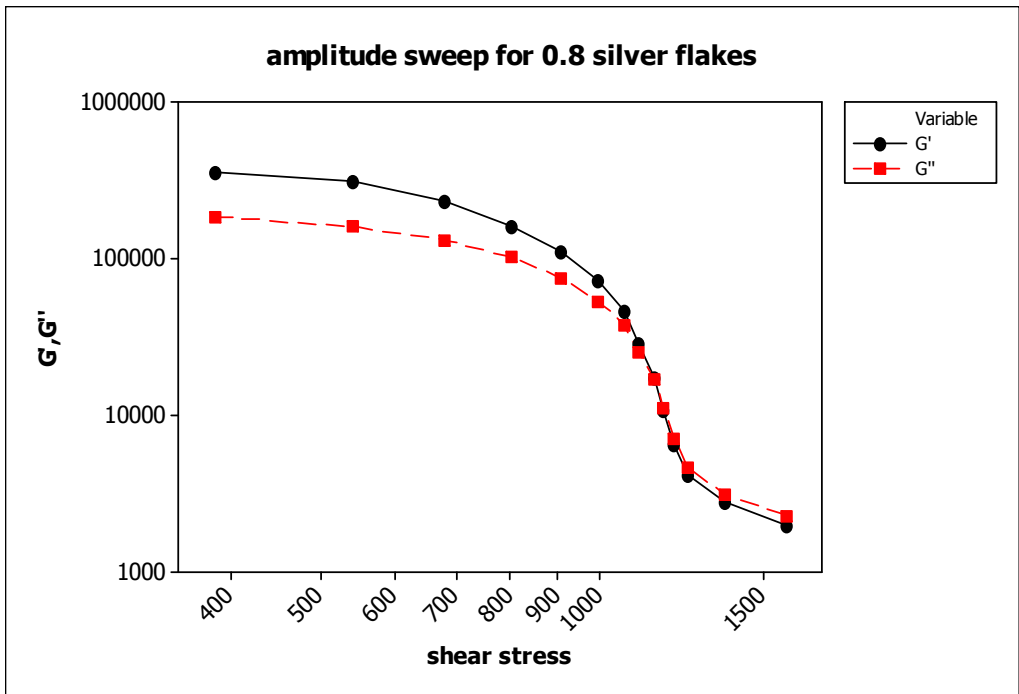


Figure 6.4 0.8wt% silver flakes

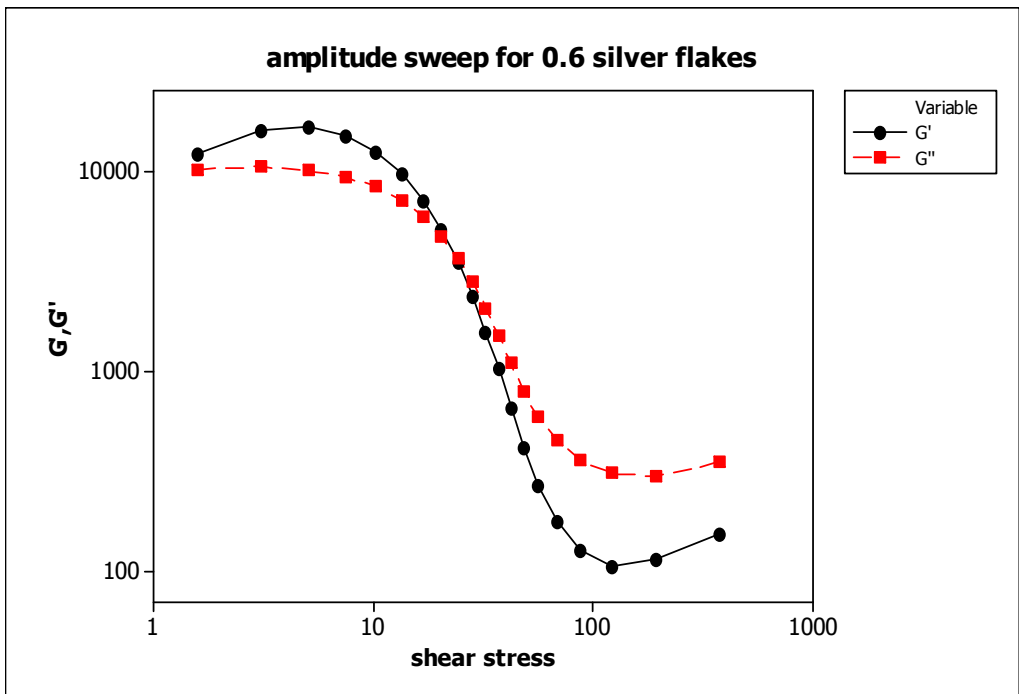


Figure 6.5 0.6wt% silver flakes

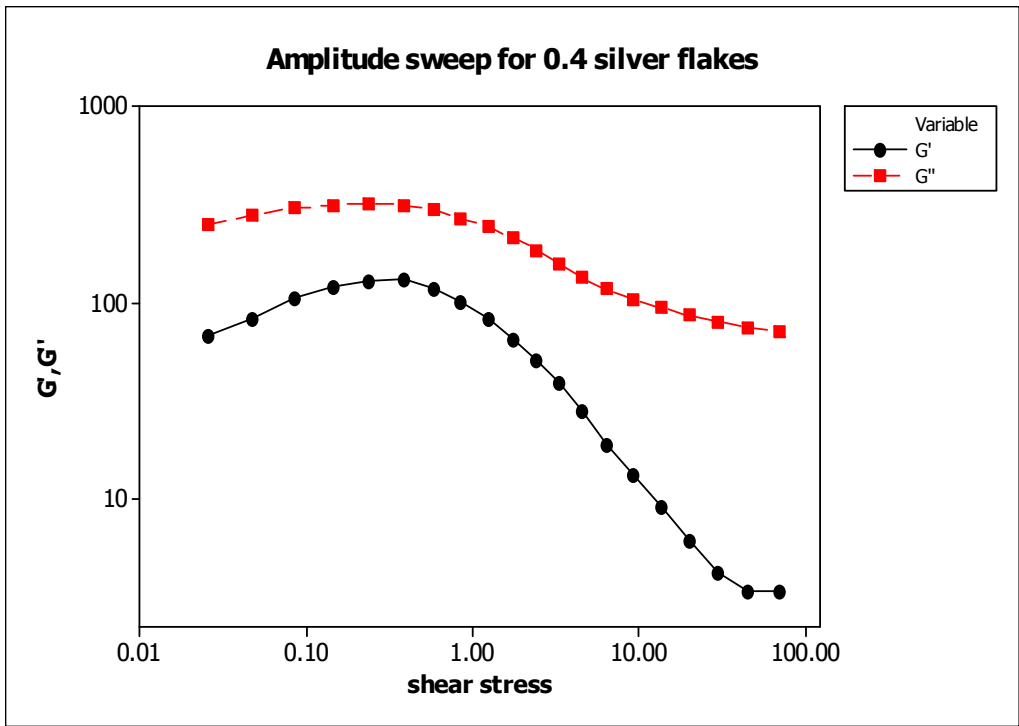


Figure 6.6 0.4wt% silver flakes

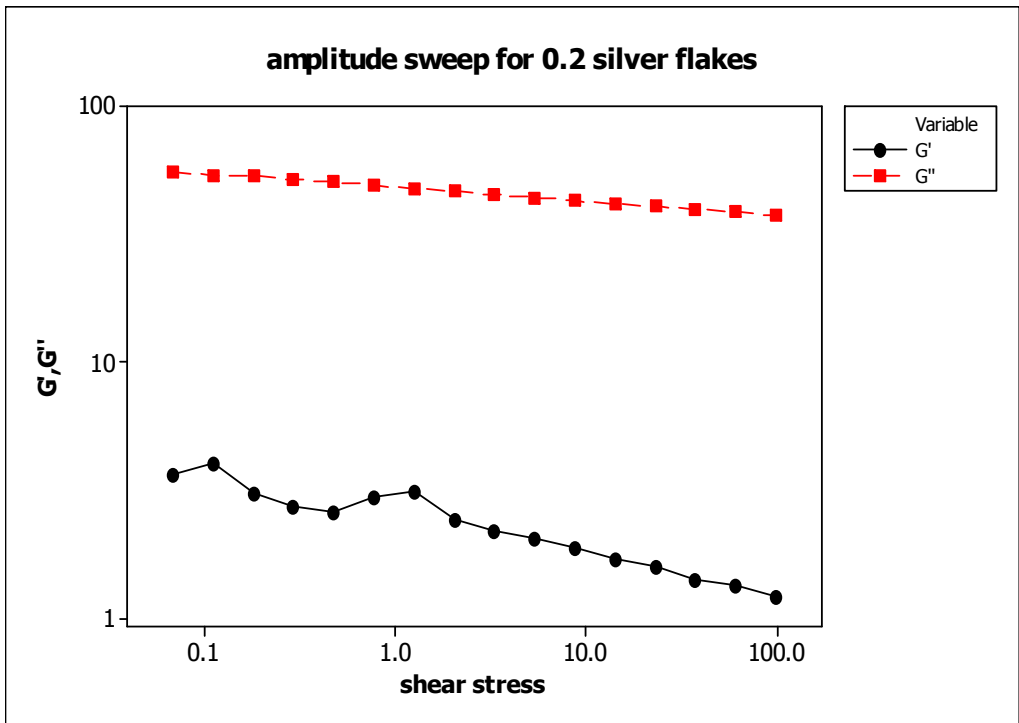


Figure 6.7 0.2wt% silver flakes

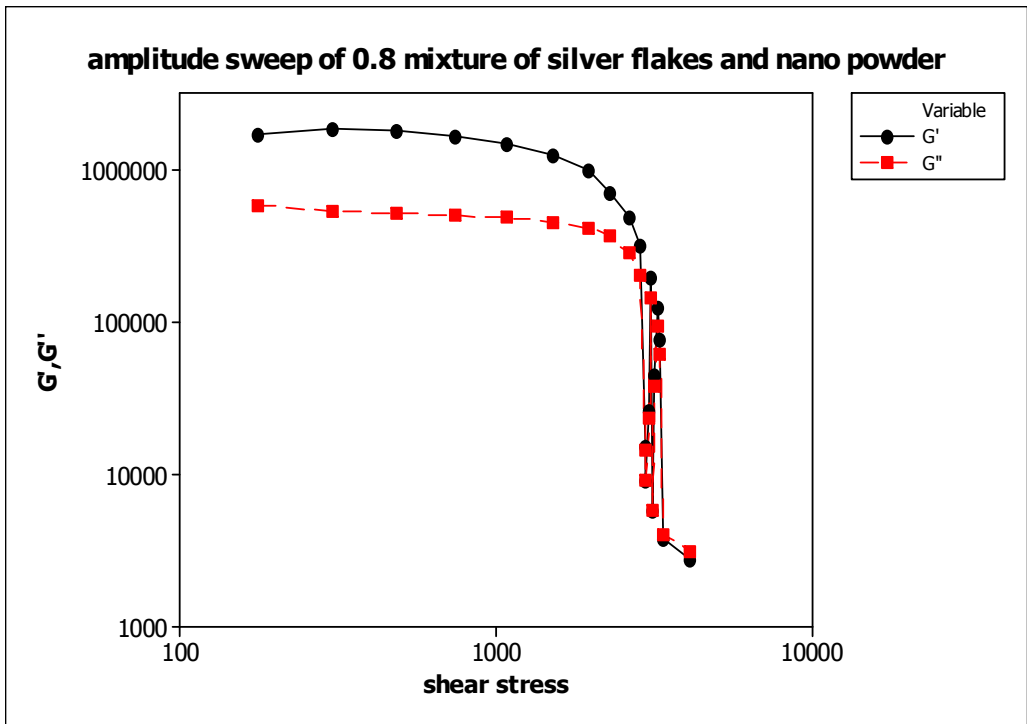


Figure 6.8 0.8wt% mixtures of silver flakes and nano-silver powder

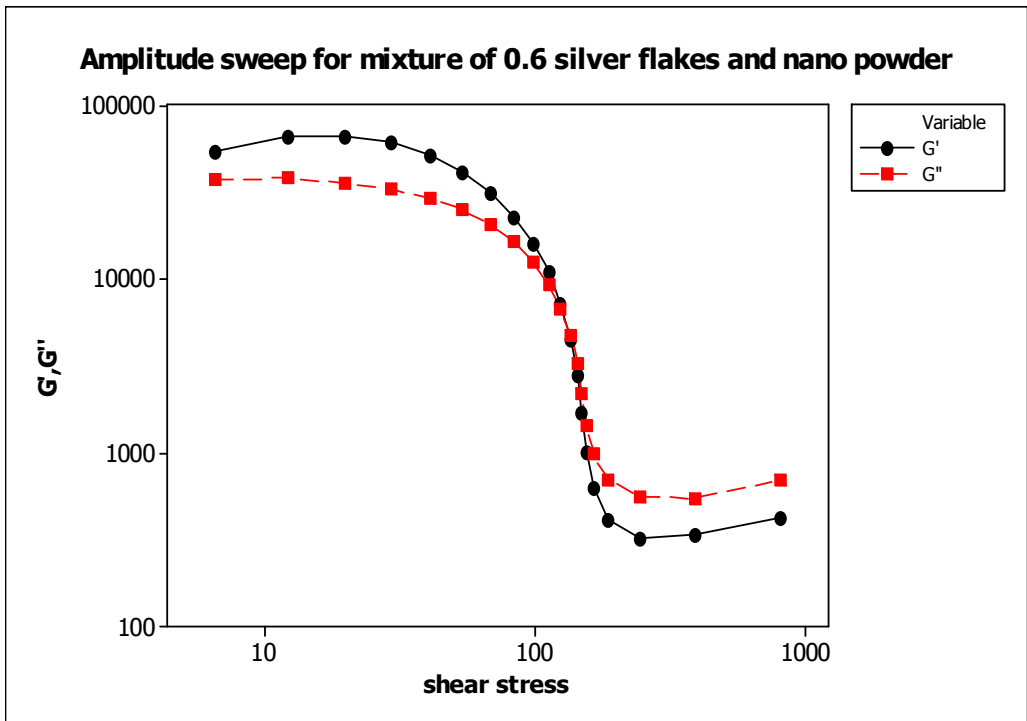


Figure 6.9 0.6wt% mixtures of silver flakes and nano-silver powder

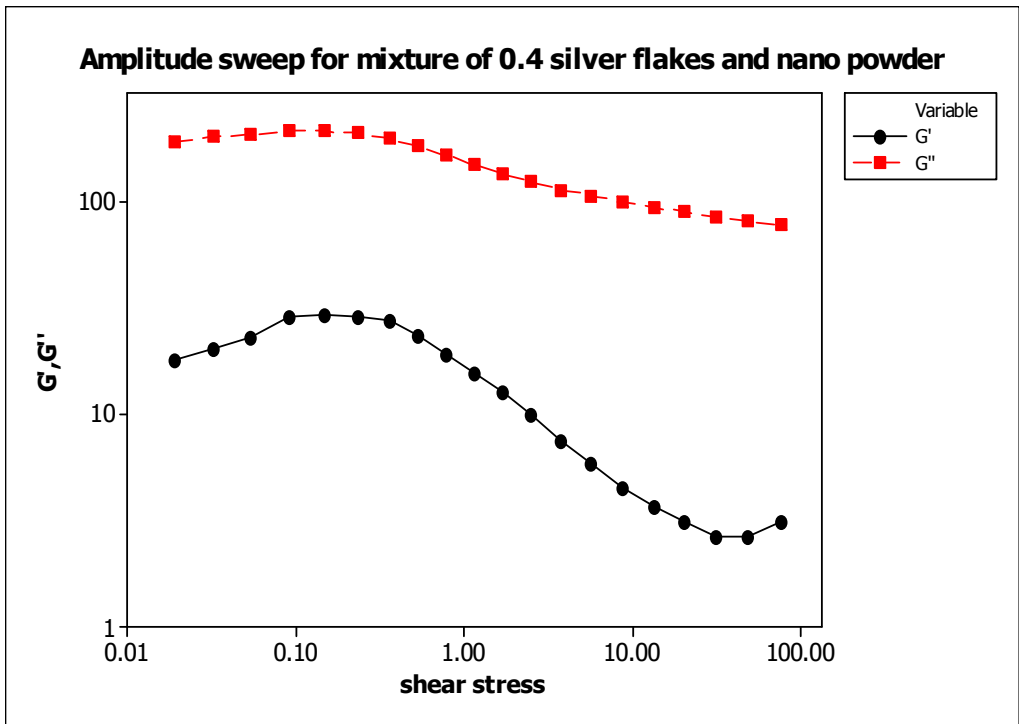


Figure 6.10 0.4wt% mixtures of silver flakes and nano silver powder

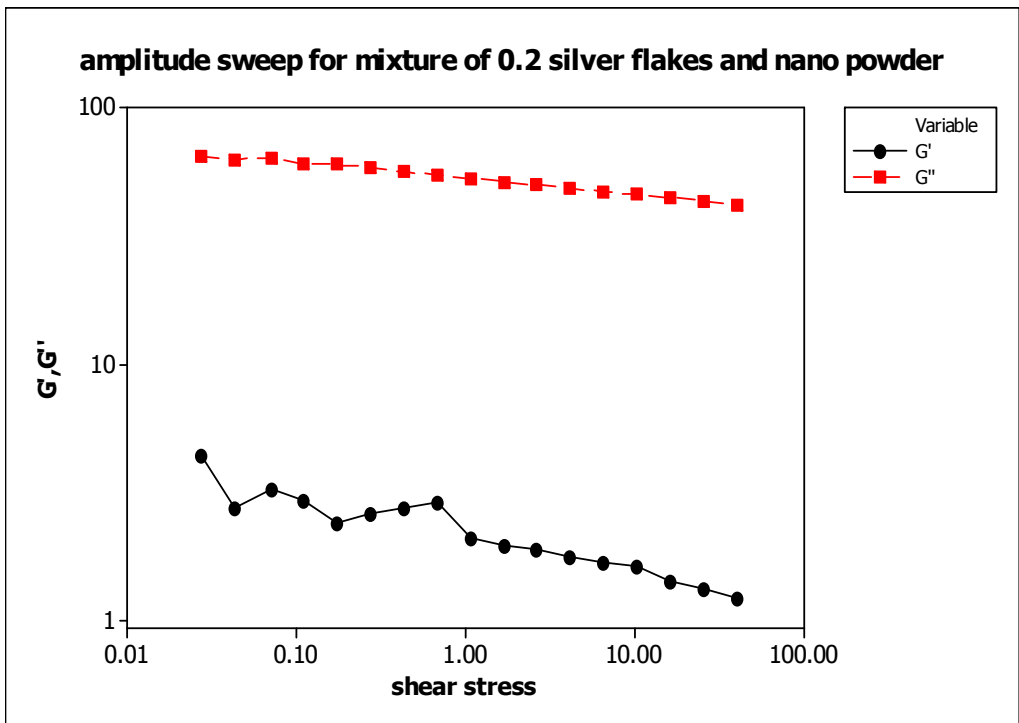


Figure 6.11 0.2wt% mixtures of silver flakes and nano silver powder

6.1.3 Correlation of oscillatory stress results to the ICAs structure

Further analysis of the elastic behaviour of the ICAs are carried out by comparing the value of storage modulus, G' and loss modulus, G'' . As we can see from the results we obtained, ICAs with 0.8wt% and 0.6wt% silver flakes and mixture of silver flakes and silver nano-powder had the storage modulus G' that is larger than loss modulus G'' . It indicated that the materials had a solid behavior before the stress applied. As the stress increased, the ICAs will slowly deform from solid to liquid behavior. As we can see at the end point of the graph that we obtained, the loss modulus, G'' is larger than the storage modulus, G' . The solid behaviors of the ICAs are affected by several factors such as the filler content of the ICAs and the size of the filler contain. As for the ICAs with 0.4wt% and 0.2wt% silver flakes and mixture of silver flakes and silver nano-powder, the loss modulus, G'' is larger than the storage modulus, G' . These results are expected as the form of the ICAs is already in liquid form before the stress applied. Therefore, there are no intersection point between storage modulus, G' and loss modulus, G'' . The next thing we will look on is the ratio of G''/G' . The ratio gives an indication of the strength of interaction within the internal structure of suspension. From the result we obtained, ICAs with 0.8wt% silver flakes and mixture of silver flakes and nano silver powder had the lowest value for G''/G' of 0.518 and 0.338, followed by the ICAs with 0.6wt% silver flakes and mixture of silver flakes and silver nano-powder with the ratio value of 0.828 and 0.682, as shown in Table 6.5 and 6.6. From the ratios, ICAs with the lower value of the ratio are more elastic in nature compared to the ICAs that had a higher value of the

ratio. The low value of the ratio also indicated that the ICAs are cohesive which quite similar to glue. As for ICAs with 0.2wt% and 0.4wt% silver flakes and mixture of silver flakes and silver nano-powder, the ratio value is higher than 1. These indicated that the loss modulus is larger than the storage modulus. Therefore, there is no changing of solid to liquid behavior in these ICAs.

For the ICAs with 0.8wt% and 0.6wt% silver flakes and mixture of silver nano-powder, the microstructure will break down from a solid to liquid behavior with increase of shear stress. From the graph that we obtained, ICAs with 0.8wt% and 0.6wt% silver flakes and mixture of silver flakes and silver nano-powder had a rapid structural breakdown after stress had increase to a certain level. It is previously thought that the small sized particles/flakes in ICAs should result in stronger interaction between the particles and the liquid medium, which result in strong paste structure. The interaction between the particles and the liquid medium within the paste microstructure is only true within the linear visco-elastic region. Beyond this region the interactive forces between the particles and liquid medium is broken down with increasing shear stress. The interaction between the particles and the resins has a direct effect on the flow behaviour of the ICAs.

Table 6.5 Oscillatory amplitude sweep parameter within the linear visco-elastic region for silver flakes

	0.2wt%	0.4wt%	0.6wt%	0.8wt%
G'(storage modulus)	1.981	6.73×10^1	1.22×10^4	3.57×10^5
G''(loss modulus)	6.76×10^1	2.47×10^2	1.01×10^4	1.85×10^5
G''/G' ratio	3.414	3.671	0.828	0.518

Table 6.6 Oscillatory amplitude sweep parameter within the linear visco-elastic region for mixture of silver flakes and silver nano-powder

	0.2wt%	0.4wt%	0.6wt%	0.8wt%
G'(storage modulus)	0	1.81	5.53×10^4	1.75×10^6
G'' (loss modulus)	6.98×10^1	1.91×10^2	3.77×10^4	5.91×10^5
G''/G' ratio	∞	10.61	0.682	0.338

The bar chart in Figures 6.12 and 6.13 above showed the value of applied shear stress at the point where the storage modulus is equal to the loss modulus for all the ICAs materials. After this intersection point, it means that the ICAs had deformed from a solid behaviour to a liquid behaviour. In the other hand, after this intersection point, the loss modulus value is larger than the storage modulus value. The stress at $G'=G''$ can be used as an indicator for assessing the cohesiveness of the paste. Consequently, the lower the stress at $G'=G''$, the more liquid-like the material is which could contribute to paste to

fracture during the aperture emptying process (Bao et al., 1998). This is the test where we know the shear stress needed in order to deform the ICAs into a liquid behaviour. A low of shear stress at $G'=G''$ cause the ICAs to fracture during the release aperture process for stencil printing leaving the paste within the aperture. From the result that we obtained, it indicated that the conductive adhesive with mixture of silver flakes and silver nano-powder had a higher shear stress compared to conductive adhesive with silver flakes only. Therefore, adding silver nano-powder into conductive adhesive will increase cohesive behaviour of the pastes.

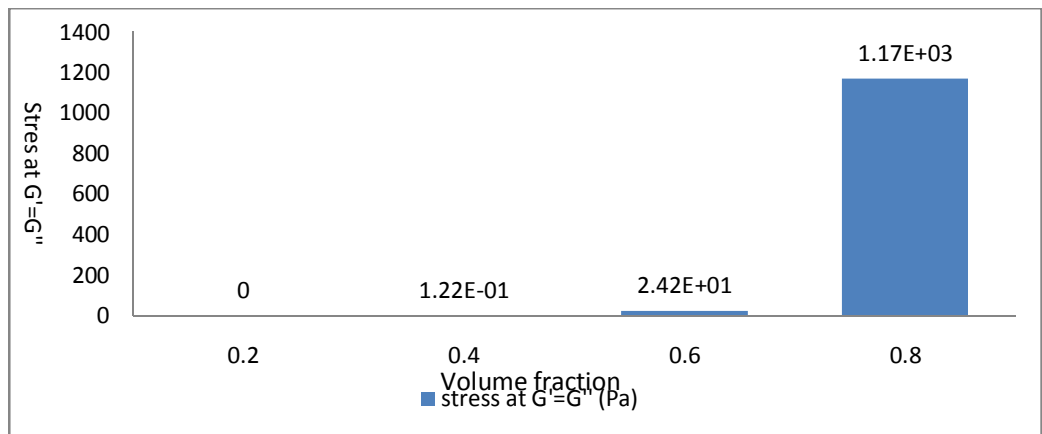


Figure 6.12 Stress where the $G'=G''$ for silver flakes

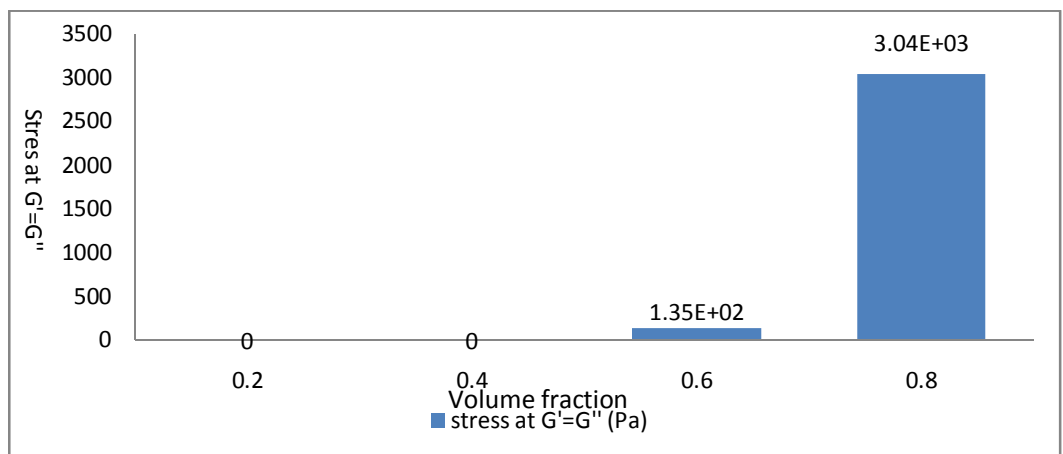


Figure 6.13 Stress where $G'=G''$ for mixture of silver flakes and nano silver powder.

6.1.4 Correlation of phase angle to quality of pastes formulation

At this discussion, we will discuss the relationship between the phase angle (δ) and the quality of the formulation of the ICAs. The phase angles are calculated from 0 degree to 90 degree. Values that are close to 0 degree indicates that the materials are in solid behaviour while values that close to 90 degree are in liquid behaviour. The ICAs are said to be tacky if the phase angle is low while it can slump easily if the phase angle value is high.

Table 6.7 Phase angle of silver flakes ICAs paste

ICA silver flakes	0.2	0.4	0.6	0.8
Phase angle (δ)	73.67	74.76	39.62	27.38

Table 6.8 Phase angle of mixture of silver flakes and silver nano-powder ICAs paste

ICA mixture of silver flakes and nano powder	0.2	0.4	0.6	0.8
Phase angle (δ)	90	84.6	34.28	18.66

The value of the applied shear stress on phase angle for all the tested ICAs is tabulated in the Table 6.7 and 6.8 above. Based on the results obtained, higher filler contain of ICAs will tend to be visco-elastic in nature. As we can see from the table, ICAs with 0.8 wt% silver flakes and mixture of silver flakes and silver nano-powder had the lowest phase angle value follow

by 0.6 wt%, 0.4 wt% and 0.2 wt%. Phase angle needed to be considered for stencil printing process as it affected the separation of the ICAs material.

Chapter 7

CONCLUSION AND FURTHER WORK

7.1 Introduction

This chapter presents the conclusions and suggestions for future work for the study carried out on the rheological characterisation of isotropic conductive adhesives (ICAs). This study on the rheological characterisation of isotropic conductive adhesives (ICAs) has three main objectives, as follows:

1. To study the effect of constant shear and hysteresis shear on the thixotropic behaviour of ICAs pastes
2. To study the paste creep deformation and recovery behaviour of ICAs pastes
3. To study the solid-like and liquid-like oscillatory shear flow behaviour of ICAs pastes

7.2 Conclusion

This conclusion section is divided into three main parts namely; the summary of study the thixotropic behaviour of ICAs, creep-recovery and the oscillatory shear flow behaviour of ICAs.

7.2.1 Study the thixotropic behaviour of ICAs

In this study, the viscosity of several pastes with different weight fraction of silver flakes and mixture of silver flakes and silver nano-powder based ICAs on the thixotropic behaviour of the sample pastes.

For the constant shear test, sample pastes containing silver nano-powder show a higher viscosity. The study shown that the sample paste which containing smaller filler particle forms stronger intermolecular bonding compare to the sample pastes without silver nano-powder.

For the hysteresis loop test study, the present of an area between the down curve and up curve shows that the sample pastes are thixotropic in nature. The results from this study show that smaller filler size leads to have large surface area and better inter-particle attraction, so that it forms stronger intermolecular bonding to resist structural breakdown. In addition, the pastes with 0.6 wt% and 0.8 wt% for both types of filler showed a recovery index less than 60% as opposed to the lower weight fraction. The presence of the liquid medium helps to facilitate the recovery of the structure after the removal of stress. The addition of the silver nano-powder improves the recovery of the pastes E and F when compared to A and B.

7.2.2 Study on the creep-recovery behaviour of ICAs

The study showed that the addition of silver nano-powder with silver flakes showed higher deformability based on the deformation index (J_2/J_1) of 1.604 for 0.8 wt% (paste E) as opposed to 1.528 for 0.8 wt% (paste A). The calculated recovery index were almost the same for paste A and E at 0.8 wt%.

It seems that the addition of the nano-powders into the silver flakes based ICAs increases the ability for the material to deform under low shear stress but it has an impact the recover of the material.

7.2.3 Study of oscillatory shear flow of ICAs

In this study, the parameter storage modulus, G' is higher than loss modulus, G'' gives a solid-like behaviour, the results shown there are true for 0.6wt% and 0.8wt%. The higher percentage of filler content provides stronger particles interaction gives a solid-like behaviour which storage modulus G' is higher than the loss modulus G'' . For 0.4wt% and 0.2wt%, loss modulus G'' is higher than the storage modulus G' . The minority of filler content in 0.2wt% and 0.4wt% sample pastes show that is very weak bond between particles.

Another parameter investigated is the yield point which is the stress at $G'=G''$, which is an important indicator of paste cohesiveness. The higher value of yield point, indicate the higher degree of cohesiveness of the pastes, which mean that the sample paste need a significant amount of stress to change from solid state to liquid state. The results obtained showed the samples paste which consist of nano silver power give a higher yield point which mean the finer particles help to provide a strong particle interaction. Hence, more stress is needed to apply for the paste release from stencil aperture during printing process.

Phase angle provides a swift way of assessing the transition from solid-like to liquid-like behaviour of the sample pastes. Among the sample pastes, 0.8wt% showed a low value of phase angle compare to other sample pastes,

and the paste is said to be high cohesive or tacky. Especially the 0.8wt% with silver nano-powder sample paste, showed the slowest phase angle 18.66° . It might be due to the high volume fraction of filler content and lead to strong particle-particle interaction.

7.3 Future work

The characterisation of the pastes and its correlation to formulation materials is a very complex task. Rheology is a way to describe the workability of an adhesive. In some situations, the viscosity of an adhesive, in other situations, can describe the rheology; the thixotropy of an adhesive is used. It is meaningless to talk about viscosity if the adhesive is thixotropic. Thixotropic materials are characterised by the fact that when not stirred they are form stable but when they are mechanically stirred, they become more or less viscous. By optimisation of the amount and the properties of the filler particles and by use of different additives it should be possible to achieve a suitable rheology for stencil printing. The results suggested that size of filler played an important role and strongly affected the viscosity of ICAs. Further work is recommended to disperse the filler with high shear technology such as three-roll mill method.

REFERENCES

Allende, M. and Kaylon, D.M. (2000) Assessment of particle-migration effects in pressure-driven viscometric flows, *Journal of Rheology*, 44/1, pp.79-90.

Amorós J.L. Sanz V. Monzo M. Beltrán V. (2001) Rheological behaviour of concentrated bimodal suspensions 1: Influence of quartz and deflocculant content on clay suspension viscosity, *British Ceramic Transactions*, 100(4), pp. 159-164.

Anderson, R., Maria, F.G. and Kolli, V.G. (1995) Solder Paste Rheology and Fine Pitch Slump, *Journal of SMT*, pp.12-18.

Aral, B.K. and Kaylon, D.M. (1994) Effects of temperature and surface roughness on time dependent development of wall slip in steady torsional flow of concentrated suspensions, *Journal of Rheology*, 38/4, pp.957-970.

Banfill, P.F.G and Saunders, D.C., (1981), On the viscometric examination of cement pastes, *Cement and Concrete Research*, 11, pp.363-370,

Barnes, H.A. (1995) A review of the slip (wall depletion) of polymer solutions, emulsions and particle suspensions in viscometer: its causes, character, and cure, *Journal Non-Newtonian Fluid Mechanics*, 56, pp.221-251.

Barnes, H.A. (1997) Thixotropy a review, *Journal Non-Newtonian Fluid Mechanics*, 70, pp.1-33.

Barnes, H.A. (1999) The yield stress-a review or 'παντα ρει'-everything flows, *Journal Non-Newtonian Fluid Mechanics*, 81, pp.133-178.

Barnes, H.A. (2000) Measuring the viscosity of large particles (and flocculated) suspensions-a note on the necessary gap size of rotational viscometers, *Journal of Non-Newtonian Fluid Mechanics*, 94, pp.213-217.

Barnes, H.A. (1989) Shear-thickening ('Dilatancy') in suspensions of non-aggregating solid particles dispersed in Newtonian liquids, *Journal of Rheology*, 33, pp.329-66.

Bao, X., Lee, N.C., Raj, R.B., Rangen, K.P. and Maria, A. (1998) Engineering solder paste performance through controlled stress rheology analysis, *Journal of Soldering and Surface Mount Technology*, 10/2, pp.26-35.

Bekkour, K and Kherfella, N (2002) Linear Viscoelastic Behavior of Bentonite-Water Suspensions, *Applied Rheology*, 12(5), pp. 234-240.

Berli, C.L., and Quemada, (2000) D.Rheological modeling of microgel suspensions involving solid-liquid transition, *Langmuir*, 16, pp.7968–7974.

Burton, R. H., Folkes, M. J., Narh, K. A., and Keller, A. (1983) Spatial variation in viscosity in sheared polymer melts, *Journal of Materials Science*, 18 (1),pp.315 – 320.

Buscall, R., McGowan, J.I. and Jones, A.J.M. (1993) The rheology of concentrated dispersions of weakly attracting colloidal particles with and without wall slip, *Journal of Rheology*, 34/4, pp. 621-641.

C.H. Mangin, (1991) “Where quality is lost on SMT boards,” *Circuit Assembly*,

Carpenter, B., Pearsall, K. and Raines, R. (1994) Predicting Printability of WSPs through Rheological Characterisation. In: *Proceeding of IEEE/CPMT, US*, pp. 1082-1088.

Caufin, B. and Papo, A, (1984) Rheological behaviour of Cement Pastes, *Zement-Kalk-Gips*, 12, pp.656-661

Cross, M.M. (1965) Rheology of non-Newtonian fluids: A new flow equation for pseudoplastic systems, *Journal of Colloid Science*, 20, pp.417-437.

Costello B. (1997) The use of creep tests after pre-shear to predict the sagging and slumping properties of Multicore Solders.

Darby, R. (1986) Hydrodynamics of slurries and suspensions. In: N.R. Cheremisinoff ed., *Encyclopedia of Fluid Mechanics*, Gulf Publishing, Houston, TX, Vol. 5, pp. 49-91.

Durairaj, R., Ekere, N. N., and Salam, B. (2004). Thixotropy flow behaviour of solder and conductive adhesives paste. *Journal of Material Science: Materials in Electronic*, 15, 677

Durairaj, R., Mallik, S., Seman, A., Ekere, N. N. (2008). *Viscoelastic properties of solder paste and isotropic conductive adhesives used for flip chip assembly*. Malaysia : 33rd International electronics manufacturing technology conference (IEMT).

Durairaj, R., Mallik, S., Seman, A., Marks, A., and Ekere, N. N. (2009). Rheological characterisation of Sn/Ag/Cu solder paste. *Journal of Materials and Design*, 30, 3812-3818

Durairaj, R., Mallik, S., Seman, A., Marks, A., and Ekere, N. N. (2009), "Rheological characterisation of solder pastes, isotropic conductive adhesives used for flip chip assembly," *Journal of Materials and Processing Technology*, **209**, 3923.

Durairaj, R., Nguty, T.A. and Ekere, N.N. (2001) Critical factors affecting paste flow during stencil printing of solder paste, *Soldering & Surface Mount Technology*, 13/2, pp.30-34.

Durairaj, R., Jackson, G.J., Ekere, N.N., Glinski, G., Bailey, C. (2002), Correlation of solder paste rheology with computational simulations of the stencil printing process, *Soldering and Surface Mount Technology*, 14 (1), pp.11-17

Eilers H.(1941), “Die Viskosität von Emulsionen hochviskoser Stoffe als Funktion der konzentration”, *Kolloid-Zeitschrift*, **97**, 313-321 .

Einstein A.(1906), “Über die von der molekularkinetischen Theorie der Wärme geforderte Bewegung von in ruhenden Flüssigkeiten suspendierten Teilchen”, *Ann. Phys.*, **17**, 549-560

Ekere, N.N. and He, D. (1996) The performance of vibrating squeegee in the stencil printing of solder pastes, *Journal of Electronics Manufacturing*, 6/4, pp.261-270.

Ekere, N.N. and He, D. (1998) The viscoelastic characteristics of solder paste under high frequency oscillatory shear. In: *Proceeding of 23th IEEE/Int. Electronic Manufacturing Technology Symposium, 1998, Austin, Texas, USA*

Fan, Q., Cui, H., Fu, C., Li, D., Tang, X., Yuan, Z., Ye, L., Liu, J.(2011), “The effect of functionalized silver on rheological and electrical properties of conductive adhesives,” *ECS Transactions*, 34, pp. 811-816.

Ferguson, J. and Kemblowski, Z. (1991) *Applied Fluid Rheology*. Elsevier Applied Science, London.

Franco, J.M., Gallegos, C. and Barnes, H.A. (1998) On slip effects in steady-state flow measurements of oil-in-water food emulsions, *Journal of Food Engineering*, 36, pp.89-102.

Frazier, J., Enno, R. and Ables, W. (1990) The design of a simple few component water-soluble flux solder paste. In: *2nd Intl. Flux Conference on Flux Technology*, September 1990, pp.1-13.

Ghezzehei T. A. and Or, Dani. (2001) Rheological properties of wet soils and clays under steady and oscillatory stresses. *Soil Science Society of American Journal*, 65, pp.624-637.

Gevgilili, H. and Kaylon, D.M. (2001) Step strain flow: Wall slip effects and other error sources', *Journal of Rheology*, 45/2, pp.467-475.

Hahn, S.L., Ree, T. & Eyring, H. (1959). Flow mechanism of thixotropic substances. *Industrial and Engineering Chemistry*, 51, 856–857.

Haslehurst, L. and Ekere, N.N. (1996) Parameter interactions in stencil printing of solder pastes, *Journal of Electronics Manufacturing*, 6/4, pp.307-316.

Herschel, W.H. and Bulkley, R., (1926), *Kolloid-Z*, XXXIX, pp.291, in, Skelland, A.H.P., (1967), '*Non-Newtonian Flow and Heat Transfer*', John Wiley and Sons, Inc. New York.

Herschel, W.H. and Bulkley, R., (1926), 'Measurement of consistency as applied to rubber-benzene solutions', *Proc. Am. Soc. Test. Mat*, XXVI, pp. 621, in, Skelland, A.H.P., (1967), '*Non-Newtonian Flow and Heat Transfer*', John Wiley and Sons, Inc. New York

Heymann, Lutz, Peukert, Sigrid and Aksel, Nuri (2002) On the solid-liquid transition of concentrated suspensions in transient shear flow, *Rheologica Acta*, 41 (4), pp. 307–315.

Ho, Li-Ngee, Wu, TengFei, Nishikawa, Hiroshi, (2013), "Properties of Phenolic-Based Ag-Filled Conductive Adhesive Affected by Different Coupling Agents," *Journal of Adhesion*, Vol 89, pp. 847-858.

Hwang, J.S. (1989) *Solder paste in electronics packaging*, Van Nostrand Reinhold, New York.

H.W. Lin, C.P. Chang, W.H. Hwu and M.D. Ger, (2008), "The rheological behaviours of screen-printing pastes," *Journal of Materials Processing Technology*, 197, 284-291.

- Irfan, M., and Kumar, D., (2008) "Recent advances in isotropic conductive adhesives for electronics packaging applications," *International Journal of Adhesion & Adhesives*, Vol 28, pp. 362-371
- Jackson, G.J., Durairaj, R. and Ekere, N.N., (2002) Characterisation of Lead-Free Solder Pastes for Low Cost Flip-Chip Bumping. In: *International Electronics Manufacturing Technology (IEMT)*, San Jose, CA, USA.
- Jirinec, M.J. (1984) Characterisation of Solder Paste for Surface Mount Attachment. In: *Proceedings of Circuit Expo*, pp.43-48.
- Johnson, C.C. and Kevera, J. (1989) *Solder Paste Technology: Principles and Applications*, TAB Books Inc.
- Joshi, Y.M., Lele, A.K. and Mashelkar, R.A. (2000) A unified slip model, *Journal of Non-Newtonian Fluid Mechanics*, 94, pp.135-149.
- Kalousek, G.L. (1973) A new instrument for measuring thixotropy, *Cement Concreter Research*, 3, pp.315-23.
- Kaylon, D.M., Yaras, P. and Yilmazer, U. (1993) Rheological behaviour of a concentrated suspension: A solid rocket fuel simulant, *Journal of Rheology*, 37/1, pp.35-53.
- Kalyon, D. M. (2005) Apparent slip and viscoplasticity of concentrated suspensions, *Journal of Rheology*, 49(3), pp.621-640.
- Kardashian, V.S. and Vellanki, S.J.R. (1978) A Method for the Rheological Characterization of Thick-Film Pastes, *IEEE Transactions on Components, Hybrids, and Manufacturing Technology*, 2/2, pp.232-239.
- Kim, H.K. and Shi, F.G. (2001) Electrical reliability of electrically conductive adhesive joints: dependence on curing condition and current density, *Journal of Microelectronics*, 32, pp.315-321.

Kolli, V.G., Gadala-Maria, F. and Anderson, R., (1997) Rheological characterisation of solder paste for surface mount applications, *IEEE Transactions on Components, Packaging and Manufacturing Technology, Part B*, 20/4, pp.416-423.

Lapasin, R. (1994) Rheological Characterisation of Solder Pastes, *Journal of Electronic Materials*, 23/6, pp.525-532.

L. Haslehurst and N.N. Ekere, (1996), "Parameter interactions in stencil printing of solder pastes," *Journal of Electronics Manufacturing*, 6/4, 307

Li, D.; Cui, H. Chen, S., Fan, Q., Yuan, Z., Ye, L., Liu, J., (2011), "A highly conductive bimodal isotropic conductive adhesive and its reliability," *ECS Transactions*, 34, pp. 583-588.

Liu, J. (1999) *Conductive adhesives for electronics packaging*, Electrochemical Publications.

Lu, D. and Wong, C.P. (1999) Effect of shrinkage on conductivity of Isotropic Conductive Adhesives (ICAs), *International Journal of Adhesion and Adhesives*, 22, pp.189-193.

Lu, D., Tong, Q.K. and Wong, C.P. (1999) A study of lubricants on silver flakes for microelectronics conductive adhesives, *IEEE Transactions on Components, Packaging and Manufacturing Technology, Part A*, 22/3, pp.365-371.

Lu, D. and Wong, C.P. (2000) Isotropic conductive adhesives filled with low-melting-point alloy fillers, *IEEE Transaction on Electronics Packaging Manufacturing*, 23/3.

Lu, D. and Wong, C.P. (1999) Mechanism Underlying The Unstable Contact Resistance of Conductive Adhesives, *IEEE Transactions on Electronic Packaging and Manufacturing*, 22/3.

Macosko, C.W. (1994), *Rheology: Principle, Measurements, and Applications*. VCH Publishers, New York.

Metzner, A.B. (1985) Rheology of suspensions in polymeric liquids, *Journal of Rheology*, 29, pp.739-75.

Mewis, J. (1979), Thixotropy – A general review. *Journal of Non-Newtonian Fluid Mechanics*, 6, pp.1-20,

Mewis, J. (1980) Rheology of suspensions. In: *Rheology*(eds G. Astarito, G. Marrucci and L. Nicolais), Plenum Publishing, New York, Vol. 1, pp.149-68.

Mindel, M.J. (1991) Solder Paste Rheology as a Function of Temperature. In: *Surface Mount International Conference and Exposition, 1991, San Jose, CA, USA*, pp.490-495.

Mooney, M. (1931) Explicit formulas for slip and fluidity, *Journal of Rheology*, 2/2, pp.210-222.

Mujumdar, A., Beris, A.N. and Metzner, A.B., (2002) Transient phenomena in thixotropic systems, *Journal of Non-Newtonian Fluid Mechanics*, 102(2), pp.157-178.

Nguty, T.A., Ekere, N.N. and Adebayo, A., (1999) Correlating solder paste composition with Stencil Printing Performance. In: *IEEE/CPMT International Electronics Manufacturing Technology Symposium*, October 18-19 1999, Austin, Texas, pp.304-309.

Nguty, T.A. and Ekere, N.N. (2000) Monitoring the effects of storage on the rheological properties of solder paste, *Journal of Materials Science: Materials in Electronics*, 11, pp.433-437.

Nguyen, H.V., Andreassen, E., Kristiansen, H., Johannessen, R., Hoivik, N., Aasmundtveit, K.E., (2013), "Rheological characterization of a novel isotropic conductive adhesive - Epoxy filled with metal-coated polymer spheres," *Materials and Design*, Vol 46, pp. 784-793.

N.N. Ekere, I. Ismail, E.K. Lo and S.H. Mannan, (1994), "Experimental study of stencil-substrate separation speed in on-contact solder paste printing for reflow soldering," *Journals of Electronics Manufacturing*, 3/1

Nguty, T.A. and Ekere, N.N. (2000) Modelling the effects of temperature on the rheology of solder pastes and flux system, *Journal of Materials Science: Materials in Electronics*, 11, pp.39-43.

N.N Ekere and D. He, (1996), "The performance of vibrating squeegee in the stencil printing of solder pastes," *Journal of Electronics Manufacturing*, 6/4

Ogata, S., Kanazawa, J. and Takei, T. (1991) A Study of the Rheology and Printability of Solder Paste, *OKI Technical Review* 136/56, pp.5-10.

Okuru, T., Kanai, M., Ogata, S., Takei, T., and Takakusagi (1993) Optimisation of solder paste Printability with laser inspection technique. In: *IEEE/CPMT International Electronics Manufacturing Symposium*, 1993, pp.157-161.

Ostwald, W., (1926), *Kolloid-Z*, 38, pp.261, in, Skelland, A.H.P., (1967), 'Non-Newtonian Flow and Heat Transfer', John Wiley and Sons, Inc.

Perret, D., Locat, J. and Martignoni, P. (1996) Thixotropic behavior during shear of a fine-grained mud from Eastern Canada, *Engineering Geology*, 43(1), pp.31-44.

Phan-Thien, N., and Safari-Ardi, M. (1998) Linear viscoelastic properties of flour-water doughs at different water concentrations, *J. Non-Newt. Fluid Mech*, 74, pp.137-150.

Phuapradit, W., Shah, N.H., Lou, Y., Kundu, S. and Infeld, M. H., (2002) Critical processing factors affecting rheological behavior of a wax based formulation, *European Journal of Pharmaceutics and Biopharmaceutics*, 53/2, pp. 175-179

Pignon, F. and Piau, J-M. (1998), Thixotropic behaviour of clay dispersions: combinations of scattering and rheometric techniques. *Journal of Rheology*, 42 (6).

Quemada D., (1997) "Rheology of concentrated disperse systems and minimum energy dissipation principle", *Rheology Acta*, **16**, 82-94

Ramaswamy, H.S. and Basak, S., (1992) Time dependent stress decay rheology of stirred yogurt, *International Dairy Journal*, 2/1, pp. 17-31.

Roeck, M. (2000) Isotropically Conductive Adhesives for Electronic Manufacture of Flexible Printed Circuit Boards, *Electronic Packaging Technology Conference*, pp.327-334.

Roman, J.W. and Eager, T.W. (1992) Low stress die attach by low temperature transient liquid phase bonding, *Proceedings of the ISHM*, pp.52-57.

Roy, D.M. and Asaga, K (1979) Rheological properties of cement mixes: The effects of mixing procedures on viscometric properties of mixes containing superplasticizers. *Cement and Concrete Research*, 9, pp.731-739.

Russel, W.B. (1980) Review of the role of colloidal forces in the rheology of suspensions, *Journal of Rheology*, 24, pp.287-317

Rutgers, LR. (1962) Relative viscosity of suspensions of rigid spheres in Newtonian liquids, *RheologicaActa*, 2, pp.202-10

Rysard, K. and Andrzej, M. (2000) Electrically conductive adhesives in SMT – the influence of adhesives composition on mechanical and electrical, *IMAPS Poland Conference 2000*.

S.H.Mannan, N.N. Ekere, I. Ismail and M.A. Currie, (1994) “Computer simulation of solder paste flow part II: dense suspension theory,” *Journal of Electronics manufacturing*, 4

S. Mallik, N. N. Ekere, A. E. Marks, A. Seman and R. Durairaj (2010) Modelling the structural breakdown of solder paste using the structural kinetic model, *Journal of Materials Engineering and Performance*, Volume 19, Issue 1, pp. 40-45

Stoops, B. (1994) ‘Precision application of low solids flux with ink jet technologies. In: *International Conference on Solder Fluxes and Paste*, June, pp.1082-1-13.

Tattersall, G.H. and P.F.G. Banfill, (1983) *The rheology of fresh concrete*, Pitman Advanced Publishing, Inc., Boston

T. Okuru, M. Kanai, S. Ogata, T. Takei and Takakusagi, (1993), “Optimisation of solder paste printability with laser inspection technique,” *IEEE/CPMT International Electronics Manufacturing Symposium*,

Turbini, L.J. (1992) Water soluble fluxes. In: *Proceeding of NEPCON WEST*, 3, 1992, pp.1687-1695.

Usui, H., (1995), A Thixotropy model for coal-water mixtures, *J. Non-Newtonian Fluid Mech.* 60, pp.259-275.

Vand, V. (1948) Viscosity of solutions and suspensions. I, *J. Phys. Chem. Colloid Chem.*, 52, 277-99.

Vand, V. (1948) Viscosity of solutions and suspensions. II, *J. Phys. Chem. Colloid Chem.*, 52, pp.300-14.

Verreet, G. and Berlamont, J. (1988) Rheology and non-newtonian behaviour of sea and estuarine mud, in *Encyclopedia of Fluid Mechanics* (ed. N.P. Cheremisinoff), Gulf Publishing, Houston, TX, Vol. 7, pp.135-49.

Warwick, M. (1990) Towards an ideal solder cream formula, *Electronic Manufacture and Test*.

Wang, S.H. (1999) Molecular transitions and dynamics at polymer/wall interfaces: Origins of flow instabilities and wall slip, *Advances in Polymer Science*, 138, pp.229-275.

Weltman, R.N. (1943). Breakdown of thixotropic structure as a function of time. *Journal of Applied Physics*, 14, 343–350.

Whorlow, R.W. (1980) *Rheological Techniques*, Horwood Ltd., Chichester

Wildmoser, H., Scheiwiller, J. and Windhab, E.J. (2004) Impact of disperse microstructure on rheology and quality aspects of ice cream, *Lebensmittel-Wissenschaft und-Technologie*, 37 (8), pp.881-891.

Winnefeld, F. (2002) Rheological behavior of portland cement pastes during early hydration, *24th International. Conference on Cement Microscopy*, San Diego, USA.

Wong, C.P., and Lu, D. (2000) Development of solder replacement isotropic conductive adhesives, *International Symposium on Electronic Materials and Packaging 2000*, pp.304-312.

Xiao, M., Lawless, K.J. and Lee, N.C. (1993) Prospects of Solder Paste in Ultra Fine Pitch Era, *Proceedings ISHM*, pp.69-85.

Ye. L., Lai. Z and Liu, J. (1999) Effect of Ag particle size on electrical conductivity of isotropic conductive adhesives, *IEEE Transactions on Electronics Packaging Manufacturing*, 22/4, pp.299-302.

Yilmazer, U. and Kaylon, D.M., (1989) Slip effects in capillary and parallel disk torsional flows of highly filled suspensions, *Journal of Rheology*, 33/8, pp.1197-1212.

Yoshimura, A and Prud'homme, R.K., (1988) Wall slip corrections for coquette and parallel disk viscometer, *Journal of Rheology*, 32/1, pp.53-67.